

### 3.8.1 H<sub>2</sub>O on metals

#### List of acronyms and symbols used in this chapter

$\Delta\phi$	work function change
$\theta$	coverage in fractions of a bilayer
(hkl)	specific lattice plane
2D	two-dimensional
3D	three-dimensional
AES	Auger electron spectroscopy
DFT	density functional theory
ESDIAD	electron stimulated desorption ion angular detection
FTIR-RAS	fast fourier transform infrared-absorption spectroscopy
HAS	Helium atom scattering
HREELS	high resolution electron energy loss spectroscopy
IWB	intact water bilayer
IRAS	infrared reflection absorption spectroscopy
IV-LEED	intensity vs. voltage LEED measurements
LEED	low energy electron diffraction
ML	monolayer
MO	molecular orbital
NEXAFS	near-edge X-ray absorption fine structure
NRA	nuclear reaction analysis
PDB	partially dissociated bilayer
RAIRS	reflection absorption infrared spectroscopy
$S$	sticking probability or sticking coefficient
SE	secondary emission
SERS	surface enhanced Raman spectroscopy
SEXAFS	surface enhanced X-ray absorption fine structure
SFG	sum frequency generation
SHG	second harmonic generation
STM	scanning tunneling microscopy
TPD	temperature programmed desorption
UHV	ultrahigh vacuum
UPS	ultraviolet photoelectron spectroscopy
XPS	X-ray photoelectron spectroscopy

#### 3.8.1.1 Introduction

Water as the most abundant chemical species on earth plays an important role in many fields. Three quarters of the globe are covered by the oceans. The atmosphere contains water in significant amounts up to 4 vol %. The influence of water on the climate is obvious and manifested in different appearances such as fog, clouds or rain and even more solid consistencies as snow, hail or ice dependent on the atmospheric pressure and temperature. Also organic materials, including the human body consist mainly of water. Finally, minerals may contain substantial amounts of water, e.g. as crystal water. Hence knowledge about the chemical and physical behaviour of water is of fundamental importance.

Besides this natural abundance, water exhibits an enormous importance for various technical processes. First of all, it is widely used as a solvent for different mainly chemical applications. Especially electrochemistry makes use of the unique properties of water. Water is also involved in etching, galvanic and corrosion processes. Common to the latter is that water gets into contact with solid often metallic surfaces. Hence, the characterisation of the chemical interaction of water with metal surfaces is important

for the understanding and optimization of these reactions. Consequently, adsorption studies under UHV conditions are performed. Although certain objections exist with regard to the transferability of the results, these measurements allow the characterisation of adsorbed layers under well defined conditions. The whole arsenal of surface sensitive methods has been applied to get information about the thermodynamic, structural, electronic, vibrational or chemical properties of the adsorbed water layers.

The physical properties of an isolated water molecule are listed in Table 1 together with a schematic geometric model of the molecule, shown in Fig.1 [87Thi]. The shape of the molecule is determined by the sp<sup>3</sup> hybridization between the three 2p oxygen orbitals and the 1s orbitals of the two H atoms. The resulting H-O-H bonding angle of 104.5° is close to the ideal tetrahedral angle of 109.5°. The redistribution of charge from the hydrogen atoms to the oxygen leads to a relatively large dipole moment of 1.83×10<sup>-18</sup> esu cm (1.8 D, 6.14×10<sup>-30</sup> Cm) pointing from the oxygen to the hydrogen. This dipole moment is responsible for the solvation capability of water for ions in solutions, which has important consequences in electrochemistry.

The water molecule is chemically relatively stable as indicated by the dissociation energy of 498 kJ/mol (5.18 eV). Two types of intermolecular bonding mechanisms can be distinguished, H bonding and covalent bonding via the two oxygen lone pair orbitals. Both have to be taken into account upon water adsorption on surfaces. Intermolecular bonding happens by H-bonding in the liquid and the solid state. While in liquid water only irregular H bonded networks of water molecules exist, crystalline ice is constructed by a periodic arrangement of water molecules connected by H bonds to each other. The resulting crystal structure is characterised by a net of buckled hexagons within a bilayer of two hexagonal layers shifted into the threefold hollow site with respect to each other and separated by 0.48 Å in height [76Wha]. Successive bilayers follow with a unit cell edge of 6.35 Å corresponding to an O-O distance of 2.76 Å. H-bonding does not only occur among water molecules but also between water and other chemical species providing the acidic and basic group, respectively. Covalent chemical bonding through the H atom is rare. Instead, bonding of water molecules to surfaces is mostly accomplished via the two oxygen lone pair orbitals. This results in a redistribution of charge with a net transfer of charge to the surface. Consistently a work function decrease is observed. The strength of H bonding within ice and covalent bonding of water molecules to metallic substrates is comparable with the consequence that clustering of H bonded water molecules often occurs even at very low coverage. Water monomers are only observed at low adsorption temperatures due to the low diffusion barriers for water molecules on metal surfaces. Andersson et al. were the first who identified isolated water molecules on Cu(100) and Pd(100) at 10K [84And]. On other surfaces, water monomers have been found at defects such as steps or coadsorbed with alkali metals [95Bau].

At higher temperature, the molecules usually produce a bilayer on the surface with a similar structure as crystalline ice. This is followed by three-dimensional ice condensation. If the H-bonds are stronger than the metal-water-bonds, three-dimensional growth occurs even before the surface is completely covered by an ice bilayer. Besides molecular adsorption of water, dissociation into OH or H can be triggered by the metal. In some cases, one even finds that dissociation products and molecularly adsorbed water coexist on the surface.

In 1987 a comprehensive review about the interaction of water with solid surfaces has been published by Thiel and Madey [87Thi] revisited by Henderson [02Hen] who added the experimental results found until 2001. The present chapter summarizes the data for water adsorption on single crystal metal surfaces, based on these two review papers and complemented by results published since then. A collection of data for water adsorption on semiconductors is given by Jaegermann and Mayer in section 3.8.2 of this Landolt-Börnstein subvolume III/42A, part 4 [04Jae]. According to the general scheme of the current subvolume "Adsorbed Layers on surfaces" only data for adsorbed water in the monolayer regime on structurally and chemically well-defined crystalline metal surfaces will be presented. The importance of H-bonding between adsorbed water molecules requires a modified definition of a monolayer, i.e. the saturation coverage of the first adsorbed bilayer is regarded as a monolayer. Surface reactions between water and other adsorbates will not be considered here. Only the reactivity of the individual metal surface upon water adsorption will be dealt with. Besides molecularly physisorbed or chemisorbed water molecules, reaction products such as OH or H have to be taken into account. The interaction of these species, formed either directly via dissociative adsorption or by consecutive heating of the adsorbed layer, with coadsorbed molecular water will be described.

Within this chapter, the collected experimental data are ordered in paragraphs describing different physical and chemical quantities. This allows a convenient comparison of the properties of different metal substrates.

### 3.8.1.2 Electronic structure

The electronic structure of adsorbed water molecules is characterized by their resulting molecular orbitals, vibrations and work function changes.

#### 3.8.1.2.1 Valence band orbitals and core levels

The 1s<sup>1</sup> hydrogen and the 2s<sup>2</sup> and 2p<sup>4</sup> oxygen valence orbitals participate in the chemical binding within the water molecule. Together with the oxygen 1s<sup>2</sup> derived orbital, five occupied molecular orbitals can be classified by symmetry: (1a<sub>1</sub>)<sup>2</sup>, (2a<sub>1</sub>)<sup>2</sup>, (1b<sub>2</sub>)<sup>2</sup>, (3a<sub>1</sub>)<sup>2</sup>, (1b<sub>1</sub>)<sup>2</sup>. Contour plots of the latter four molecular orbitals together with the first two unoccupied orbitals, (4a<sub>1</sub>)<sup>0</sup> and (2b<sub>2</sub>)<sup>0</sup> are shown in Fig. 2 as given by Jorgensen and Salem [73Jor]. While the 'a' denoted MO's reflect the c<sub>2v</sub> symmetry of the water molecule, the 'b' MO's exhibit the orbital plane as the only symmetry element. Whereas the (1a<sub>1</sub>)<sup>2</sup> and (1b<sub>1</sub>)<sup>2</sup> are nonbonding, the (1b<sub>2</sub>)<sup>2</sup> is of antibonding character. In contrast the (3a<sub>1</sub>)<sup>2</sup> and (2a<sub>1</sub>)<sup>2</sup> are partly bonding and partly antibonding. Energetically these MO's can be divided into valence orbitals ((1b<sub>2</sub>)<sup>2</sup>, (3a<sub>1</sub>)<sup>2</sup> and (1b<sub>1</sub>)<sup>2</sup>) and core levels ((1a<sub>1</sub>)<sup>2</sup> and (2a<sub>1</sub>)<sup>2</sup>). The valence orbitals 3a<sub>1</sub> and 1b<sub>1</sub> are directly involved in the chemical bonding resulting in the so called 'chemical shift' of the core levels. The energetically well separated first unoccupied 4a<sub>1</sub> orbital plays a major role for the dissociation of water.

Fig. 3 shows photoelectron spectra for all five occupied molecular H<sub>2</sub>O orbitals adsorbed on a Pt(111) surface as measured with X-rays. The excitation energies are  $h\nu = 1253.6$  eV and  $h\nu = 120$  eV for the core level and the valence band region, respectively. The binding energies of the three valence MO's should be characteristic for the chemical interaction of water with metal surfaces and are listed in Table 2. Since these values are typically referred to the Fermi level, they can not be directly compared to the gas phase ionization potentials of 18.5 eV (1b<sub>2</sub>), 14.7 eV (3a<sub>1</sub>) and 12.6 eV (1b<sub>1</sub>) which are related to the vacuum level [74Rab]. Instead, one has to correct these values by adding the work function and possible relaxation energies. Nevertheless relative shifts may indicate which orbital is mainly involved in the chemical bonding. However, Henderson showed that a clear correlation does not exist for the observed energy spacings between 1b<sub>2</sub> and 3a<sub>1</sub> or 1b<sub>1</sub> orbital [02Hen]. While for water monomers the bonding via the oxygen lone pair orbital dominates, hydrogen bonding to the surface has been observed for water molecules at the rims of molecular clusters, in addition. More recently, structure models with alternating metal-oxygen and metal-hydrogen bonds have been proposed for water bilayers on Pt(111) [02Oga] and Ru(0001) [03Den] (Fig. 15). Although the molecular structure reflects the bonding configuration, changes in the binding energies do not directly allow conclusions on the exact bonding mechanism.

On the other hand, a distinction between molecularly adsorbed water and possible reaction products, such as OH can be made in a more straightforward manner. In the valence band regime OH can be distinguished from molecular water by its two orbital structure built up by the 1 $\pi$  and 3 $\sigma$  orbital with ionization energies of 8.3 eV and 12.3 eV although overlapping may complicate the identification [77Con, 85Kis].

In general the O1s core level spectroscopy does not only allow the identification of the adsorbed species but also a quantification of the amount of adsorbed H<sub>2</sub>O, as seen in Fig. 3 for increasing water exposure. Table 3 summarizes O1s binding energies for molecularly adsorbed H<sub>2</sub>O on the metal single crystal surfaces studied so far. While the identification of a single peak in the binding energy range above 532.2 eV as molecularly adsorbed water is relatively straightforward, double peak structures as observed for Ru(0001) are discussed controversially in the literature [04And, 04Wei, 91Pir]. Previously, Pirug et al. proposed a layer dependent binding energy of 531.3 eV and 532.7 eV for molecular H<sub>2</sub>O in the first and the second layer of a bilayer [91Pir]. Lateron, Andersson showed that molecularly adsorbed water gives rise to only one O1s peak at 533.0 eV for H<sub>2</sub>O and D<sub>2</sub>O as shown in Fig. 4 a and c. The second peak at

530.8 eV results from X-ray induced dissociation of water leaving hydroxyl species on the surface (Fig. 4 b and d) [04And]. At the same time, Weisenrieder published O1s spectra for water (H<sub>2</sub>O or D<sub>2</sub>O) clearly showing a double peak structure with peaks at 531.0 - 530.8 eV and 532.7 - 532.3 eV explained by the formation of a stable wetting layer consisting of OH and H<sub>2</sub>O (Fig. 5 a) in a 3:5 proportion (Fig. 5 b) [04Wei]. Both interpretations are based on experimental and theoretical findings. Whereas the “intact water bilayer” (IWB) is supported by recent findings in second harmonic sum frequency (SFG) vibrational spectroscopy by Denzler et al. [03Den] and density functional theory (DFT) performed by Michaelides et al. [03Mic], the “partially dissociated bilayer” (PDB) agrees with a low energy electron diffraction (LEED)-IV structure analysis by Held and Menzel for D<sub>2</sub>O on Ru(0001) [94Hel1] and ‘ab initio’ calculations based on DFT by Feibelman [02Fei, 04Fei, 05Fei]. Although the theoretical studies report consistently that the PDB is thermodynamically more stable than the IWB, the calculated activation energy for dissociation of about 0.5 eV is of the same order as the activation energy for desorption favoring the IWB model at low enough temperatures.

Concerning the application of electron spectroscopies, special care has to be taken in order to exclude beam induced changes in the adsorbed layer. Another controversy exists for water adsorption on Ni(110) [94Pir]. Pirug et al. resolved the broad O1s peak for a saturated H<sub>2</sub>O layer with a c(2×2) LEED pattern into almost equal contributions at 533.2 eV and 531.6 eV originating from molecular H<sub>2</sub>O and OH, respectively. Together with a saturation coverage of one O atom per surface Ni atom a bilayer structure consisting of an oxygen bonded first OH layer and hydrogen bonded second H<sub>2</sub>O layer has been proposed. This interpretation is supported by photoelectron diffraction [94Pir] and X-ray absorption fine-structure measurements in the extended (SEXAFS) and near-edge region (NEXAFS) [94Pan] but in contradiction to a single molecular layer of H<sub>2</sub>O with a saturation coverage of 0.5 O atom per Ni surface atom proposed by Callen et al. based on a coverage calibration by nuclear reaction analysis (NRA) [90Cal, 92Cal2] and the missing OH stretch frequency using fast Fourier transform ir-absorption spectroscopy (FTIR) [91Cal].

### 3.8.1.2.2 Molecular vibrations

The intra- and intermolecular bonding, as well as the bonding to the substrate upon adsorption of water can be studied applying vibrational spectroscopy. The isolated H<sub>2</sub>O molecule belongs to the  $c_{2v}$  symmetry group and exhibits 3 internal vibrations as shown in Fig. 6a. Adsorbed on surfaces the restriction of the 3 translational and 3 rotational degrees of freedom leads to 3 additional librational and 3 frustrated translational modes (Fig. 6b). Besides conventional methods such as infrared absorption spectroscopy (IRAS) [94Oga], fast Fourier transform infrared spectroscopy (FTIR), reflection absorption infrared spectroscopy (RAIRS) [02Haq], surface enhanced Raman spectroscopy (SERS), second harmonic generation (SHG), sum frequency generation (SFG), elastic and inelastic He atom scattering (HAS) [99Gle], high resolution electron energy loss spectroscopy (HREELS) and more recently scanning tunneling spectroscopy [02Kom] can be applied under UHV conditions.

Compared to all other methods which have specific restrictions, HREELS can be applied in the most universal manner [01Jac1]. The accessible frequency range is practically not restricted ranging from 20 cm<sup>-1</sup> to more than 4000 cm<sup>-1</sup> covering the frustrated molecule-substrate vibrations, inner layer lattice vibrations and all intramolecular vibrations. Making use of different excitation mechanisms, such as dipole and impact scattering, and surface selection rules, water layers can be characterized with respect to their clustering behaviour. The characterisation ranges from monomers over dimers to clusters and well ordered bilayers, local and long-range bonding configurations and the chemical composition [82Iba]. Table 4 contains data gained with all methods listed above.

Fig. 7 shows a typical sequence of HREEL spectra recorded at increasing coverage of molecular water on Pt(111) [95Bau]. The vibrational signature with losses at 3380 cm<sup>-1</sup> (O-H stretch), 1630 cm<sup>-1</sup> (H-O-H symmetric bending, “scissor”) and a broad peak at 500 - 800 cm<sup>-1</sup> (frustrated librations) indicates that H<sub>2</sub>O is molecularly adsorbed. The appearance of a loss at 240 cm<sup>-1</sup> was assigned by Sexton to a translational mode parallel to the surface ( $T_{\parallel}$ ) representing an oscillation of the whole molecule in an ice-like layer [80Sex]. Lateron, the presence of this mode was taken as an indication for the presence of ice-

like layers [87Thi]. However, Jacobi et al. showed recently that this mode belongs to a perpendicularly hindered translation ( $T_{\perp}$ ) [01Jac1] in agreement with recent HAS findings [99Gle]. Glebov et al. detected frustrated translational vibrations at even lower energy of 22 cm<sup>-1</sup>, 28 cm<sup>-1</sup> and 47 cm<sup>-1</sup> for H<sub>2</sub>O monomers, dimers and bilayer clusters, respectively. Due to the observed isotope shift between H<sub>2</sub>O and D<sub>2</sub>O these modes could be assigned to vibrations of the water molecules parallel to the surface.

The higher resolution and sensitivity of modern HREELS spectrometers allow the identification of water monomers adsorbed in chains at the upper step edges on Pt(111) at very low coverages even at 85 K. As shown in Fig. 8, monomers are characterized by a very soft frustrated-translational mode  $T_{\perp}$  at 15 meV (121 cm<sup>-1</sup>) and two frustrated-rotational modes  $L_1$   $L_2$  at 28 meV (226 cm<sup>-1</sup>) and 36 meV (290 cm<sup>-1</sup>). In addition, two bending modes  $\delta_{am}$  and  $\delta_{bm}$  can be observed, which can only be dipole active for tilted H<sub>2</sub>O molecules.

The chemical interaction between adsorbed water molecules and the substrate due to H-bonding is reflected by the observed OH-stretch vibrations. As shown in Fig. 9 Ogasawara et al. reported significant changes in this frequency range with increasing coverage [94Oga]. D<sub>2</sub>O monomers can be clearly distinguished by their reduced D-H stretch frequency of 2477 cm<sup>-1</sup> from H-bonded water clusters and ice-like layers with an O-H stretch frequency of about 2556 cm<sup>-1</sup> and 2539 cm<sup>-1</sup>, respectively. The additional peak observed at 2731 cm<sup>-1</sup> is ascribed to free OD bonds in ice in agreement with earlier findings by Ibach et al. for the hexagonally reconstructed Pt(100) surface [80Iba].

### 3.8.1.2.3 Work function changes

As listed in Table 1 the isolated water molecule exhibits a static dipole moment  $\mu = 1.83 \times 10^{-18}$  esu cm (1.8 D,  $6.14 \times 10^{-30}$  Cm) pointing from the oxygen to the hydrogens. Therefore characteristic changes in the work function are expected upon adsorption of molecular water depending on the orientation of this dipole. In addition the transfer and polarization of charge due to the chemical bonding of the water molecule to the metal surface should influence the observed work function change. In general a decrease in work function is observed for molecularly adsorbed water as shown for Pt(111) in Fig. 10 [85Kis]. From the linear slope at small coverages an initial dipole moment of  $\mu = 0.38$  D has been determined. This decrease in work function is consistent with a dipole orientation with a perpendicular component to the surface. In principal this should indicate, that the water molecules are adsorbed via the oxygen atoms upright standing or tilted within or with the molecular plane by less than 90°. This simple explanation does not hold in view of structure models assuming more or less flat lying water molecules [94Hel1]. Hence a more refined interpretation of the work function changes is required including charge transfer and polarization effects as shown theoretically by Bonzel et al. [87Bon].

As shown in Fig. 11 for D<sub>2</sub>O adsorption on Ni(110), the work function change depends on the adsorption temperature [90Cal]. This behaviour can be explained by the condensation of water at 130 K. At 180 K condensation is no longer possible. Instead the formation of a first chemisorbed layer with a sharp c(2×2) LEED pattern is observed. The minimum in the  $\Delta\Phi$  curve of 970 mV corresponds to a coverage of  $\Theta=0.38$ , while a saturation value of 780 mV is reached at  $\Theta=0.48$  according to the given coverage calibration. Discrete changes during desorption upon annealing as shown by a comparison of work function measurements with thermal desorption spectroscopy in Fig. 12 allow a detailed structural interpretation. The two desorption states  $A_2$  and  $A_1$  corresponds to molecularly adsorbed D<sub>2</sub>O with different dipole moments of 1.93 D and 0.58 D, respectively. While the  $A_1$  peak has been related to the desorption of molecularly adsorbed D<sub>2</sub>O from c(2×2) structure, the  $A_2$  peak has been explained by a decomposition of OD-D<sub>2</sub>O complexes, which results from D<sub>2</sub>O dissociation at temperatures above 205 K. Worthwhile to note, that this interpretation is at variance with structure models published by Benndorf and Madey [88Ben] and Pirug et al. [94Pir], as mentioned above. Work function changes have been measured for a number of single crystal metal surfaces as listed in Table 5, based on the data collection presented by Jacobi in section 4.2 of this Landolt-Börnstein subvolume III/42A, part 2 [01Jac2] and completed by some new results published since then.

The work function of water covered surfaces has also some importance with respect to electrochemistry [95Stu, 95Tra]. The equivalence between the work function measured in UHV and the potential of zero charge under electrochemical conditions justifies UHV model experiments concerning the electrochemical double layer [86Stu, 98Pir].

### 3.8.1.3 Dissociative versus molecular adsorption

A further important question concerning H<sub>2</sub>O adsorption on metal surfaces is, whether it adsorbs as a molecule or whether it dissociates. This topic has been discussed in detail by Thiel and Madey [87Thi] and new results have been added by Henderson [02Hen]. Mostly, TPD, vibrational spectroscopy and photoemission have been used to deduce the chemical species present on the surface [87Thi]. But also other techniques such as isotope exchange [80Bow, 81Net, 82Ben, 84Nyb, 84Stu] or work function measurements [01Jac2, 82Her1, 82Her2, 88Her] provide information on the chemical species. Thiel and Madey have outlined that a first approach based on thermodynamic properties, in particular the enthalpy gain of the reaction, is rather successful in predicting dissociation. Thus, in many cases, kinetic barriers appear to be of minor importance. Most surfaces prefer a dissociative adsorption, but some group VIII and group IB metals lead to molecular adsorption. The use of thermodynamic parameters appears to be safe as long as the enthalpy difference between molecular and dissociative state is larger than 100 kJ/mol with the exception of Zn.

This results in some borderline cases such as Co, Ni, Re, Ru and Cu, where the dissociation depends critically on the particular surface and/or the step density. Since minute amounts of oxygen, other adsorbates or intrinsic defects, e.g. step edges, can trigger the dissociation, some of these cases are still controversial as discussed in the previous section. Interestingly, the structure of the H<sub>2</sub>O-layer itself can lead to dissociation. Held et al. concluded from detailed measurements that domain boundaries of the ice bilayer on Ru(0001), which exhibit a different H<sub>2</sub>O-density, are stabilized by dissociation [95Hel1, 95Hel2]. Based on DFT calculations, Feibelman even proposed that the ice bilayer itself on Ru(0001) is stabilized by dissociating 2/5 of the molecules [02Fei, 03Fei, 05Fei].

An activated dissociation has been shown to occur on Ni(110) [89Gri, 94Pir, 96Kas] and Pt(111) [97Wan, 99Kin], in the latter case induced by adsorption of hyperthermal H<sub>2</sub>O. The dissociation can also be favored by the use of a high pressure ( $> 10^{-6}$  mbar) atmosphere of H<sub>2</sub>O as has been shown on Au(111) [75Che] and C(0001) (graphite) [92Chu, 93Chu]. Moreover, the application of an electric field of the order of 0.5 V/Å can lead to dissociation as has been shown on Pt tips [00Sco, 98Sco, 99Pin]. Thus, a direct transfer of dissociation data obtained in UHV to environments involving higher pressure, liquids or applied fields has to be taken with care.

Table 6 summarizes the results concerning dissociation of H<sub>2</sub>O on crystalline metal surfaces in UHV. For comparison the differences in enthalpy taken from Thiel and Madey are indicated [87Thi]. The first number compares the cases of complete dissociation with molecular adsorption assuming an adsorption energy of 50 kJ/mol independent of the substrate. The second number compares partial dissociation, i.e. formation of OH and O with molecular adsorption. The minus sign means that dissociation is favored.

Recently, the dissociation of H<sub>2</sub>O on metal surfaces by electrons, photons and ions has been investigated in more detail. This is reviewed by Henderson, where the additional dissociation channels either triggered by ionization or by activation of the adsorbed molecule are described [02Hen].

### 3.8.1.4 Geometric structure of molecularly adsorbed ice

#### 3.8.1.4.1 Adsorption geometry

It is generally believed that H<sub>2</sub>O prefers an on-top adsorption site with the oxygen binding to the surface atom [87Thi]. This is largely concluded from DFT calculations and has been confirmed by experiments on Ru(0001) [94Hel1], Pd(111) [04Cer] and Ni(110) [94Pan] by LEED-IV measurements, STM and SEXAFS measurements, respectively. As outlined by Thiel and Madey, this can be understood by

regarding H<sub>2</sub>O as an electron donor with respect to the metal, which prefers to sit on sites of relatively low electron density on the metal surface [87Thi]. This idea is in accordance with the preferential adsorption of H<sub>2</sub>O at the upper edge of steps [96Mor] and the fact, that desorption temperatures of molecular H<sub>2</sub>O are enhanced on the rougher single crystal surfaces [87Thi] having stronger corrugation in electron density for H<sub>2</sub>O adsorption and, thus, providing positions of lower electron density. DFT calculations give a more detailed picture. Basically, the occupied orbitals 3a<sub>1</sub>, 1b<sub>1</sub>, and 1b<sub>2</sub> of H<sub>2</sub>O hybridize with unoccupied d-orbitals of the metal including a charge transfer from H<sub>2</sub>O to the metal. Since H<sub>2</sub>O gets closer to the d-orbitals at positions of low sp-electron density, the binding is stronger at these positions [85Bau].

The orientation of the water molecule with respect to the surface normal has been studied for several metals as Ru(0001) [77Mad, 82Doe, 94Hel2, 95Hel2], Cu(110) [83Mar], Cu(100) [86Nyb], Pd(100) [86Nyb], Ni(110) [85Nöb], Ni(111) [94Pan] and Ni(665) [87Nöb]. The orientation has been concluded from work function changes presuming a certain dipole moment of the water molecule, from electron stimulated desorption patterns (ESDIAD), from NEXAFS, from polarization dependence of photoemission yields and from the angular distribution of HREELS yields. Generally, it has been found that the H<sub>2</sub>O-molecule is tilted significantly with respect to the surface normal. The molecule is even parallel to the surface for Ni(111) [94Pan] and Ru(0001) [94Hel2, 95Hel2], and has a tilt angle of 57°-58° on Pd(100) and Cu(100) [86Nyb]. ESDIAD studies on Ru(0001) have shown that the azimuthal angle of the tilted molecule is random at low coverage presumably due to the presence of monomer H<sub>2</sub>O and gets ordered with six-fold symmetry at higher coverage presumably due to the formation of a hydrogen-bonded network [77Mad, 82Doe].

Recent XPS results and DFT calculations indicated that besides the oxygen bonding to the metal an additional hydrogen-metal bond is formed in bilayers on Pt(111) [02Oga] and Ru(0001) [02Fei, 04And, 04Wei]. In the latter case, DFT calculations even found that a partial dissociation of the H<sub>2</sub>O takes place leaving 3/5 of the molecules intact [02Fei, 05Fei]. However, this topic is still controversial.

#### 3.8.1.4.2 Binding energy and desorption temperatures

The strength of the H<sub>2</sub>O-metal bond is difficult to determine. It is mostly concluded from TPD. Generally, two peaks originating from the desorption of ice multilayers and the ice bilayer on top of the metal are observed. However, since ice on metal surfaces forms islands including hydrogen bonds, the identification of the desorption temperature of the bilayer with binding energy is not straightforward. A detailed picture of the desorption kinetics is required, which has only partly been settled. Nevertheless, typical values for the deduced oxygen-metal binding energy are about 50±15 kJ/mol [87Thi]. A more detailed analysis performed on Ag(110) results in a binding energy of 60±1 kJ/mol [89Wu].

Besides the bilayer and multilayer peak, additional peaks can be found at higher temperature. They are assigned to H<sub>2</sub>O bound to special defects as e.g. step edges, and to recombinative desorption of dissociation products, respectively [02Hen, 87Thi]. The latter assignment requires information from other techniques as e.g. UPS in order to proof that dissociation takes place on the surface.

On the most noble surfaces as Au and Ag as well as on Cu(111), only a single peak is found which shifts to higher temperatures at higher coverage (see references in Table 7). This indicates that the binding to the metal is weaker than the binding within the ice layer. The result makes sense, since the d-shell of Ag, Au and Cu is largely filled reducing the density of empty d-levels for binding. On these surfaces, the ice grows in three-dimensional hydrogen-bonded clusters on the surface.

Fig. 13 shows the typical cases of TPD spectra [87Thi]. Only a multilayer TPD peak is observed on Ag(110). A multilayer and a bilayer peak are observed on Pt(111). Ru(0001) exhibits the exceptional behaviour, that two bilayer peaks are observed in addition to the multilayer peak as discussed below. Finally, Ni(110) shows multilayer and bilayer peak and, in addition, two peaks originating from desorption of molecules presumably stabilized by dissociation products and from recombinative desorption, respectively.

Table 7 lists measured TPD peak temperatures of ice adsorbed on different metal surfaces. They are ordered with respect to their assignment. The slight deviations of peak temperature in different

experiments on the same substrate can be due to different heating rates, partly different initial coverages and different adsorption temperatures. An uncertainty in the temperature calibration cannot be ruled out either. With regard to these uncertainties, the original values have been partly rounded to a 5 K scale. Since it is usually assumed that the ice multilayer desorbs at the same temperature on each surface, it might be helpful to relate the other peaks to the multilayer peak. Note that the TPD peaks often shift with coverage and, thus, the given desorption temperatures are typical values only. If possible, they are given at the same H<sub>2</sub>O coverage, i.e. the bilayer peak is given at a coverage of about half a bilayer and the multilayer peak at a coverage of about 2 bilayers.

Generally, the desorption temperatures are higher for the rougher surfaces of the same material, which fits with the idea that water is an electron donor bound most tightly to positions of low electron density of the metal.

Interestingly, a relation between desorption temperature and lattice mismatch between ice(0001) and the hexagonal metal surfaces has been found by Thiel and Madey (Fig. 32 of [87Thi]). The highest desorption temperature exists on Ru(0001), where the ice lattice is expanded by 3% with respect to pure ice. The desorption temperatures get increasingly smaller if the lattice mismatch deviates from the 3% value in both directions.

However, since the H<sub>2</sub>O bilayer desorption on Ru(0001) is unusual exhibiting two TPD bilayer peaks, while the D<sub>2</sub>O bilayer on Ru(0001) shows only one bilayer peak, the conclusion has to be taken with care [95Hel1, 95Hel2]. In addition, more recent TPD spectra e.g. from Pt(111) do not fit into this simple picture [02Haq].

Recently, the two TPD peaks of H<sub>2</sub>O on Ru(0001) have been correlated with a domain structure of the bilayer, which exists for H<sub>2</sub>O but not for D<sub>2</sub>O [82Doe, 95Hel1, 95Hel2]. The H<sub>2</sub>O domain boundaries transform from being H<sub>2</sub>O enriched to being H<sub>2</sub>O deficient at the temperature of the first TPD peak. Held et al. suppose that the domain boundaries may be stabilized by fragments of dissociated H<sub>2</sub>O. An influence of dissociation on this surface has also been found by DFT calculations of Feibelman, who, however, proposes a homogeneous dissociation of 2/5 of the molecules in the D<sub>2</sub>O bilayer [02Fei, 05Fei]. Indeed, recent XPS studies have shown that 3/8 of the D<sub>2</sub>O and the H<sub>2</sub>O molecules are dissociated after adsorption at 145 K [04Wei]. In contrast, Anderson found no dissociation using a slightly different preparation at 150 K, but a clear onset of dissociation at 180 K [04And]. Thus, the topic of the isotope effect on Ru(0001) is still controversial. Interestingly, the isotope effect has only been studied on Ru(0001), although Jo et al. found two bilayer peaks after D<sub>2</sub>O adsorption on Pt(111) [91Jo] while other authors studying H<sub>2</sub>O adsorption on Pt(111) find only one peak [02Haq].

#### 3.8.1.4.3 Trapping and sticking

As pointed out by Henderson, trapping and sticking is determined from different measurements [02Hen]. The trapping coefficient corresponds to the part of molecules which is not reflected by the surface, while the sticking coefficient  $S$  excludes also the molecules which are trapped by the surface but desorb prior to the measurement. The trapping coefficient is measured by molecular beam techniques, while the sticking coefficient is deduced from measurements performed after the adsorption as TPD, photoemission, AES, STM or others. Molecular beam measurements of H<sub>2</sub>O trapping on metals are rare, but as outlined by Thiel and Madey the sticking coefficient is already close to unity, if adsorption temperatures well below the desorption temperature of H<sub>2</sub>O are used [87Thi]. Moreover, the sticking coefficient at low temperature does not depend on coverage implying that trapping and sticking coefficients are similar. Exact values for the sticking coefficient are difficult to deduce due to uncertainties in the determination of the exposure and the coverage and will not be listed here. The published values are between 0.6 and 1, i.e. close to unity [87Thi]. Measurements using a well defined molecular beam for exposure (Au(111) [89Kay], Ru(0001) [97Smi], Ni(110) [90Cal], Pt(111) [02Haq]) and a well calibrated measure for coverage always give a value of  $S > 0.95$ . Also in the other measurements, the sticking is found to be independent of coverage in the temperature range between 100 K and 140 K, i.e. below the onset of significant multilayer desorption [87Thi]. Table 8 of Thiel and Madey summarizes some of the results concerning sticking.



#### 3.8.1.4.4 Diffusion and formation of small clusters

Adsorption of H<sub>2</sub>O partly leads to vibrational frequencies, which have been interpreted in terms of H<sub>2</sub>O monomers. The assignment is not always unambiguous, i.e. the features are partly interpreted as due to very small clusters as dimers or tetramers.

Fig. 9 shows vibrational spectra (IRAS) observing the transition from isolated monomers to clusters as a function of D<sub>2</sub>O coverage on Pt(111) ( $T=84$  K) [94Oga]. The features at around  $1200\text{ cm}^{-1}$  and  $2500\text{ cm}^{-1}$  are assigned to the D-O-D scissor mode and the O-D stretch mode, respectively. Both modes consist of two peaks. The lower frequency peak dominates at low coverage, while the higher frequency peak dominates at higher coverage. One deduces that the low frequency peaks correspond to the unperturbed vibrations, while the high frequency peaks are caused by stiffer vibrations due to O-D bridge bonds within ice clusters. The exact peak frequencies, thus, can be used to assign the species present on the surface. However, the assignment becomes more intricate, if one has to decide, whether monomers or dimers are present. Additional information can be gained by using ESDIAD or UPS as reviewed by Thiel and Madey and Henderson [02Hen, 87Thi].

Recently, also He scattering [97Gle, 99Gle] and STM [02Mit, 02Mor2, 04Cer, 96Mor, 97Ike] have been used to deduce the size of the adsorbed clusters. Figures 14 a-c show STM images of H<sub>2</sub>O monomers, small H<sub>2</sub>O clusters and the complete ice bilayer adsorbed on Pd(111) [02Mit], Ag(111) [03Mor] and Pt(111) [97Mor], respectively. Here, the assignment is rather direct.

Table 8 summarizes the assignments with respect to measurement temperature and coverage for the different surfaces. The existence of monomers has been deduced for Al(111), Cu(100), Cu(110), Cu(111), Ni(110), Pd(100), Pd(110), Pt(111), Re(0001) and Ru(0001). Some results on Ag(111), Ni(100), Ni(110), Pd(110), Pt(111), Re(0001) and Ru(0001) have been interpreted as due to dimers, tetramers or hexamers. Generally, there are three different cases, where monomers, dimers, tetramers and hexamers have been found. First, they exist at low temperatures (10-40 K), where certain diffusion processes are blocked and disappear at higher temperatures at the onset of diffusion [02Mit, 02Mor2, 97Gle, 99Gle]. Second, they exist at very low coverage probably due to sticking at defects, e.g. at step edges (e.g. [91Jac, 92Xu]). Third, they exist up to the coverage of half a bilayer, in particular on the more open surfaces as Cu(110) [82Spi] and Ni(110) [85Nöb, 94Pir], but disappear at coverages close to one bilayer. In the latter case, the most reasonable cause for the existence of monomers is the competition between hydrogen-metal bonds and H-bridge bonds within the ice. Monomers are stabilized by tilting the molecule towards the surface giving rise to H-metal interaction [94Pan]. The H-metal bonds might also be relevant in H-bridge bonded clusters as they appear on Pt(111) [02Oga] or Ru(0001) [02Fei] at higher temperature.

There is only one direct measurement of the diffusion of isolated H<sub>2</sub>O molecules performed on Pd(111) by STM (see inset of Fig. 14 a) [02Mit]. It results in a monomer diffusion barrier of 126 meV (8 kJ/mol) with a prefactor of  $10^{12}/\text{s}$ . Similar results are expected on other close-packed surfaces. For example, the onset of monomer diffusion on Pt(111) takes place at 40 K requiring a diffusion barrier of about 10 kJ/mol [99Gle]. On more open surfaces, the diffusion barriers could be significantly higher, e.g. recent DFT calculations on Al(100) give a value of about 320 meV (20 kJ/mol) [04Mic]. Diffusion measurements of multilayer water on a field-emission tip have been done, but can only provide an upper limit, giving e.g. an upper bound of 25 kJ/mol for the diffusion barrier on Pt(111) [95Bry, 97Bry, 99Bry].

#### 3.8.1.4.5 Ice bilayer

If two requirements are fulfilled, a stable bilayer of ice can be prepared on a metal surface. First, it requires the absence of dissociation at least as a major pathway (see Table 6) and second, H<sub>2</sub>O within the ice bilayer on the surface must be stronger bound than H<sub>2</sub>O within the ice multilayer, i.e. a distinct TPD bilayer peak must exist (see Fig. 13). Then, the H<sub>2</sub>O exposure at temperatures higher than the multilayer and lower than the bilayer TPD peak results in a well defined bilayer. The bilayer basically is a layer of I<sub>h</sub>-ice(0001) with half of the oxygen lone pair orbitals bound to the metal. It consists of hexagonal ice rings as depicted in Fig. 15a.

Half of the molecules bind to the metal via their oxygen lone-pair orbital and the other half is bound by H-bridge bonds to three neighbouring H<sub>2</sub>O molecules. The exact geometry of the bilayer can be different from I<sub>h</sub>-ice. In particular, it has been shown that the vertical O-O distance can be much smaller in the bilayer than in ice e.g. on Ru(0001) [94Hel1], Pd(111) [04Cer] or Pt(111) [01Jac1, 02Oga]. Reasons are the electron deficiency within the ice layer due to electron donation to the metal, but also the competition between H-bridge bonds within the ice and H-metal bonds. The latter details have only recently been realized by detailed analysis of IV-LEED [94Hel1], STM [04Cer] and XPS [02Oga] results, respectively, and have been confirmed by DFT calculations. Fig. 15 b shows the structure of the ice bilayer on Pt(111) deduced from XPS [02Oga]. In contrast to usual I<sub>h</sub>-ice, where the remaining dangling H-atom points away from the surface, the upper molecules are rotated by 180° giving rise to an additional H-metal bond. The structure of the D<sub>2</sub>O bilayer on Ru(0001) as calculated by DFT is shown in Fig. 15 c [02Fei]. Here, the dangling H-atom is abstracted giving rise to an additional O-metal bond of the resulting OH and to an additional H-metal bond at a different surface atom. However, the symmetry of the ice bilayer is still intact and the number of H-bridge bonds is the same as in a bilayer of I<sub>h</sub>-ice.

The registry of the bilayer with the metal surface is guided by the interplay between optimal adsorption site on the metal (i.e. on-top) and optimal length of the H-bridge bonds within I<sub>h</sub>-ice. Early LEED studies have mostly concluded that the periodicity of the bilayer is given by the substrate resulting in a ( $\sqrt{3}\times\sqrt{3}$ )R30° superstructure on the close-packed surfaces and a c(2×2) superstructure on the more open fcc(110)-surfaces (see Table 9). The basic idea was that the resulting stress within the ice bilayer can be relieved by buckling the H-bridge bonds [87Thi]. However, more recent, detailed studies on Pt(111) and Ru(0001) using He-scattering [97Gle], LEED [02Hag, 82Doe, 95Hel1, 95Hel2] and STM [97Mor] have shown that the structure can be more complex. On Ru(0001), the stress within the H<sub>2</sub>O bilayer resulting from the ( $\sqrt{3}\times\sqrt{3}$ )R30° superstructure is additionally relaxed by forming a regular array of stripe domains separated by domain walls every 6.5 lattice spacings of the substrate [95Hel1, 95Hel2]. Two types of domain walls exist depending on the preparation. They have either additional or missing H<sub>2</sub>O molecules with respect to the perfect ( $\sqrt{3}\times\sqrt{3}$ )R30° superstructure and are probably responsible for the two TPD peaks of the H<sub>2</sub>O-bilayer on Ru(0001). These domain walls do not exist for D<sub>2</sub>O on Ru(0001), where only one TPD peak is found. A structure with domain walls may also exist on Rh(111) as concluded from weak He diffraction spots appearing in addition to the ( $\sqrt{3}\times\sqrt{3}$ )R30° spots [00Gib].

For the bilayer on Pt(111), which exhibits a lower desorption temperature than the bilayer on Ru(0001), the H-bridge bonds seem to be of larger importance. Three different phases have been detected by STM depending on the preparation [97Mor]. One of these phases (I) realizes the optimal bridge bond length and is rotated with respect to the substrate in order to optimize the bonding positions of the O-atoms on the metal (Fig. 14c). The other two phases appear to have a similar local structure, but are less dense than phase I. They are most likely identical to the ( $\sqrt{37}\times\sqrt{37}$ )R25.3° superstructure detected by He scattering [97Gle]. Interestingly, the transformation between the different phases is mediated by a highly mobile, disordered phase which coexists with the ordered phases at higher temperature. He-scattering [97Gle] and LEED [02Hag] measurements have found a fourth superstructure, i.e. ( $\sqrt{39}\times\sqrt{39}$ )R16.1°, by preparing the bilayer at slightly lower temperature.

Due to the complexity of the superstructures, the long-range order of the ice bilayer on Ru(0001) and Pt(111) is not completely settled. However, it might even be that more complex structures also exist on other surfaces, which have been less investigated so far.

Table 9 summarizes the available results on the superstructure of the ice bilayer on different surfaces. Partly, the ice layers are prepared at temperatures below the onset of multilayer desorption, but still exhibit a ( $\sqrt{3}\times\sqrt{3}$ )R30° and a c(2×2) superstructure. However, no superstructure spots are observed on a number of surfaces including all fcc(001) surfaces. Note that the H<sub>2</sub>O adsorption on Co, Al and Zr leads to the coexistence of dissociated and molecular H<sub>2</sub>O on the surface (Table 6, Table 7), which might prohibit the long-range ordering.

#### Acknowledgements:

We gratefully appreciate that M.A. Henderson provided the text of his recent review.

### 3.8.1.5 Tables for 3.8.1

#### Organisation of the tables

**Table 1:** Physical properties of the isolated H<sub>2</sub>O molecule

**Table 2:** Valence band peak positions (in eV relative to the Fermi level, unless otherwise noted) for molecularly adsorbed water on metal surfaces

**Table 3:** O 1s XPS peak positions (in eV) for molecularly adsorbed water on metal surfaces

**Table 4:** Vibrational assignments and frequencies (in cm<sup>-1</sup>) for molecularly adsorbed H<sub>2</sub>O and D<sub>2</sub>O on metal surfaces

**Table 5:** Work function changes for molecularly adsorbed water on metal surfaces given with respect to the clean surface

**Table 6:** Assignments of molecular versus dissociative adsorption of water on crystalline metal surfaces

**Table 7:** Desorption temperatures of water from different crystalline metal surfaces ordered with respect to their assigned adsorption geometry and desorption paths, respectively

**Table 8:** Adsorption structure of water on metal surfaces

**Table 9:** Measured superstructure periodicity of ordered 2D ice bilayers on solid surfaces

**Table 1.** Physical properties of the isolated H<sub>2</sub>O molecule

Parameter	Value	Ref.
HOH bond angle, $\theta_{\text{HOH}}$	104.5°	69Eis
OH bond length, $r_{\text{OH}}$	0.957 Å	69Eis
van der Waals (hard-sphere) radius, $r_{\text{vdW}}$	1.45 Å	71Cot
moments of inertia, $I$ :		69Eis
$I_y$	$1.0220 \times 10^{-40} \text{ g}^{-1} \text{ cm}^{-2}$	69Eis
$I_z$	$1.9187 \times 10^{-40} \text{ g}^{-1} \text{ cm}^{-2}$	69Eis
$I_x$	$2.9376 \times 10^{-40} \text{ g}^{-1} \text{ cm}^{-2}$	69Eis
Dipole moment, $\mu_z$	$1.83 \times 10^{-18} \text{ esu cm}$ ( $6.14 \times 10^{-30} \text{ Cm}$ )	69Eis
mean polarizability, $J$	$1.444 \times 10^{-24} \text{ cm}^3$	69Eis
O-H bond dissociation energy, $D_0$	498 kJ/mol (5.18 eV)	71Cot

**Table 2.** Valence band peak positions (in eV relative to the Fermi level, unless otherwise noted) for molecularly adsorbed water on metal surfaces

Substrate	1b <sub>2</sub>	3a <sub>1</sub>	1b <sub>1</sub>	Temperature [K]	Reference
Al(100)	<sup>a</sup>	11.6	7.3	100	82Sza
Ag(110)	12.0	8.9	<sup>a</sup>	155	84Bar
Ag(111)	13.7 <sup>b</sup>	10.0 <sup>b</sup>	7.1 <sup>b</sup>	110	90Bla
Co(0001)	13.0	9.3	6.9	100	82Her2
Co(11 $\bar{2}$ 0)	13.5	9.9	7.3	100	82Her2
	13.0	9.4	7.4	100	94Gre

Cu(100)	13.1 <sup>b</sup>	9.1 <sup>b</sup>	6.9 <sup>b</sup>	90	85Spi2
	11.9	9.9	6.3	80	80Sas
Cu(110)	13.0	8.8	7.2	90	82Spi
	13.2	9.0	7.1	100	83Ban1, 84Ban
	12.6	8.8	6.8	90	83Mar
Ni(100)	13.0	9.3	7.0	100	84Pee
Ni(110)	12.7	9.4	6.8	150	81Ben
	13.2	9.3	7.6	137	94Pir
	12.8	8.6	6.8	150	85Nöb
Ni(111)	12.3	9.5, 8.3 <sup>d</sup>	6.3	120	89Pac, 91Bor
Ni(221)	11.7	8.9	6.7	157	98Mun
Ni(665)	12.3	8.5	6.2	120	87Nöb
Ni(775)	12.7	8.2	6.3	145	98Mun
Pt(110)-(1×2)	11.5	8.5	5.5	100	90Fus
Pt(111)	11.9	8.2	5.6	100	80Fis1, 80Fis2
	11.3	7.6	5.4	90	89Ran1
	12.0	8.1	6.0	100	85Kis
	18.6 <sup>c</sup>	14.7 <sup>c</sup>	12.6 <sup>c</sup>	100	84Lan
				120	84Lan
Pt6(111)×(100)	11.7	8.4	5.8	120	81Mil
Rh(100)	12.2	8.7	6.4	100	85Gre
Rh(111)	12.4	8.2	6.4	90	87Wag1
Ru(0001) <sup>c</sup>				95	80Thi, 81Thi, 82Thi2
	12.5	8.7	7.1	120	91Pir
Ti(0001) <sup>c</sup>				90	82Sto

a. Peak position not given or not resolved.

b. Estimated from the spectra in the paper.

c. Spectrum not shown; paper only refers to 'three peak spectrum'.

d. The 3a<sub>1</sub> is split due to the bilayer water structure.

e. Relative to the vacuum level.

**Table 3.** O 1s XPS peak positions (in eV) for molecularly adsorbed water on metal surfaces

Surface	O 1s peak energy [eV]	Temperature [K]	Reference
Al(100)	533.3	100	82Sza
Al(110)	535.0	105	94Mil
Ag(110)	533.5	80	83Au
Au(111)	533.2	110	93Laz
	532.6		94Coe
Co(110)	533.6	100	94Gre
Cu(110)	533.4	90	85Spi2
	533.4	95	03Amm
	533.5	110	89Cle
Cu(111)	533.5	80	79Au, 80Au
Ni(100)	533.5	100	84Pee
Ni(110)	533.4	100	82Ben
	533.2	180	94Pir
Ni(111)	533.2	120	93Kuc1, 93Kuc2, 94Kuc, 95Sch
NiAl(110)	533.9	123	95Gle
Ni <sub>3</sub> (Al,Ti)(100)	533.4	140	95Chi1, 95Chi2
Ni <sub>3</sub> (Al,Ti)(111)	533.3	140	95Chi1, 95Chi2

Surface	O 1s peak energy [eV]	Temperature [K]	Reference
Pb(110)	534.0	80	93Au
Pt(111)	532.2	100	80Fis1
	532.2-532.9	100	85Kis
	532.2-531.8	90	89Ran1, 89Ran2
Rh(111)	532.2	90	87Wag1, 88Wag1
Ru(0001)	533.2 and 531.3	120	91Pir
	532.7 - 532.3 (H <sub>2</sub> O)	145	04Wei
	531.0 - 530.8 (OH)		
	533.0 (D <sub>2</sub> O)	150	04And
	532.8 (H <sub>2</sub> O)		
	530.8 (OH)		

**Table 4.** Vibrational assignments and frequencies (in cm<sup>-1</sup>) for molecularly adsorbed H<sub>2</sub>O on metal surfaces, values in parentheses are for D<sub>2</sub>O

Substrate	O-H stretching	HOH bending	Libration (rocking)	Libration (wagging)	M-OH <sub>2</sub> stretching	Frustrated translation	Adsorption configuration of water	Refs
Al(100)	(2720, 2560)	(1200)						93Bus
	3695, 3510	1655	685 <sup>a</sup>		685 <sup>a</sup>	265		82Sza
Al(110)	3450	1640	780			220		94Mil
Al(111)	3450 (2590)	1650 (1210)	775 (645)					87Cro, 88Che
Ag(100)	3390	1610	870	730		240		86Din
Ag(110)	3410	1660	740			200	cluster	81Stu
	3452 (2549)	1645 (1170)	766 (581)					89Wu
	3452 (2549)	1645 (1170)	766 (581)					89Wu
Au(111)	3295	1650	835					98Pir
Cu(100)		1589 (1178)				230 (198)	monomer	84And
Cu(110)	3600, 3375, 3180	1600	745		460		low coverage	89Lac
	3350	1600	780					90Sch
	3600, 3375, 3180	1600	750				cluster	91Sas
	3350	1600	780					90Lac
	3380, 3070 (2595, 2315)	1630 (1220)	690 (545)				cluster	82Bar
Fe(100)	3470, 3000 (2595, 2315)	1630 (1220)	690 (545)				cluster	91Hun, 93Hun

Substrate	O-H stretching	HOH bending	Libration (rocking)	Libration (wagging)	M-OH <sub>2</sub> stretching	Frustrated translation	Adsorption configuration of water	Refs
Ni(110)	3350					290	cluster – low coverage	85Oll
	3660, 3350, 3030 (2670, 2450, 2140)	1610 (1110)	760 (530)	530		230 (275)	cluster – high coverage	85Oll
				800 (588)	667 (493)			98Kov
	3700 (3330)	1600	780			270	cluster	86Hoc
NiAl(110)	3620 (2660)	1620 (1200)			560 (560)		cluster – low coverage	95Gle
	3460 (2550)	1650 (1220)	760 (600)			240 (240)	multilayer	95Gle
Pb(110)	3420	1660	750			230		93Au
Pd(100)		1597 (1186)				335 (282)	monomer	84And
	3404	1605	807		613	218	cluster	84Nyb, 86Nyb
	3380	1640	810			235	cluster	84Stu
Pd(110)	3600, 3440	1610	750	660	480	215	cluster – low coverage	90Bro2
	3500, 3300 (2600, 2470)	1630, 1580 (1200, 1160)	745 (570)	660 (510)	500	215 (215)	cluster – high coverages	90Bro1, 91Bro
					403		monomer	02Kom
Pd(111)	3400 (2500)	1616 (1188)	812 (730)	642 (585)		192	cluster	91Zhu
Pt(100)	3430	1645	920	520				92Kiz
	3670, 3380, 2850 (2710, 2550)	1630 (1210)	920 (680)	560 (470)	460 (470)	240 (240)		80Iba
Pt(110)	3670, 3410	1620	730	620		270		99Che
Pt(111)	3400 (2530),	1625 (1200)	700 (550-700)		550 (500)	250 (240)		80Sex
	3445 (2543)	1625 (1195)	688 (750)		530 (510)	260 (230)		96Gil
	3680, 3430 (2700, 2560)	1630 (1195)	695 (510-580)		560	240 (240)	cluster	95Bau

Substrate	O-H stretching	HOH bending	Libration (rocking)	Libration (wagging)	M-OH <sub>2</sub> stretching	Frustrated translation	Adsorption configuration of water	Refs
Pt(111) cont.						22 (21) <sup>b</sup> 28 (27) <sup>b</sup> 47 (46) <sup>b</sup>	monomer dimer bilayer cluster	99Gle
	(2706, 2465)						monomer	99Oga
	(2641, 2577, 2492)	(1179, 1166)					dimer	99Oga
	3440	1610	670		530	240		87Wag2, 88Wag1, 88Wag2
	3350	1600	780					91Sas
	3420	1630	700		550			80Fis2
	(2730, 2535)						bilayer	95Vil
	3670, 3420	1621	1040, 928	678, 524	266	129	bilayer	01Jac1
	(2552)	(1199)					sub-bilayer	02Haq
	(2355, 2472, 2721)	(1199)					bilayer	02Haq
Pt(553)	3318						sub-bilayer, mol. chains at steps	04Gre
Rh(111)	3370 (2480)	1620 (1190)	800-400 <sup>a</sup> (600-300 <sup>a</sup> )			230 (230)	cluster	87Wag1, 88Wag1
Ru(0001)	3490	1615	740				cluster	94Shi
	3565, 3400, 2935	1520	920	700	390		cluster	84Thi
	3350	1650	890-700	460-310 <sup>a</sup>			cluster	80Thi, 81Thi, 82Thi1
	(2531)	(1157)					monomer	00Nak, 01Nak
	(2690, 2611, 2442)	(1172)					tetramer	00Nak, 01Nak
	3445 (2729, 2290, 2550)	1562					monomer	02Nak 03Den
Zn(0001)	3670, 3532, 3290	1605	850					86Sen

Substrate	O-H stretching	HOH bending	Libration (rocking)	Libration (wagging)	M-OH <sub>2</sub> stretching	Frustrated translation	Adsorption configuration of water	Refs
Zr(0001)	(2543, 2732)						cluster	97Li2
a. poorly resolved.								
b. frustrated translational vibrations parallel to the surface								

**Table 5.** Work function changes for molecularly adsorbed water on metal surfaces given with respect to the clean surface. Additionally applied experimental methods are commented together with an interpretation of the adsorption behaviour

H <sub>2</sub> O, D <sub>2</sub> O/ Substrate	<i>T</i> [K]	Method	Type	$\Delta\Phi$ [eV]	at $\theta$	Comments, interpretation	Ref.
Ag(110)	80	(Kelvin)	III	-0.65	2 L	LEED, ESDIAD, TDS no long-range order at 80 K	87Ban1
Al(100)	100	Kelvin	III	-0.95	12 L		89Mem2
	100	Kelvin	IV	-1.2	2.5 L	FT IR-RAS, NRA at 100 K	93Bus
				-0.9	16 L	no dissociation	
Co(0001)	100	Kelvin	I	-1.1	10 L	UPS, TDS	82Her2
Co(11 $\bar{2}$ 1)	100	Kelvin	I	-1.2	10 L	reversible adsorption below 300 K; $\Delta\Phi > 0$	
Co(11 $\bar{2}$ 0)		SE edge (UPS)	III	-1.3	0.7 L	XPS, UPS	94Gre
Cu(100)	10	EELS		-0.06	0.25 L	EELS, LEED	84And
	80	SE edge (UPS)		-0.8	saturation	UPS	85Spi1
	120	Kelvin	III	-0.9	10 L	HREELS, TDS defects stabilize H <sub>2</sub> O clusters	93Bro2
Cu(110)	90	SE edge (UPS)	III	-0.9	1 L	UPS, LEED, ELS	82Spi
	350	*		-0.09		*mirror electron microscopy	83Phu
	110	Kelvin	III	-0.95	4 L	LEED, UPS, TDS $\mu_0 = 0.85$ D	83Ban1, 84Ban
Cu(111)	110	Kelvin	III	-0.85	4 L	LEED, UPS, TDS $\mu_0 = 0.5$ D	83Ban1
Ir(110)-(1×2)	140	Diode	III	-0.7	1 L	TDS, XPS	81Wit
Ni(100)	100	SE edge (UPS)		-1.05	sat.	UPS, XPS, TDS	84Pee
Ni(110)	150	Kelvin	III	-0.7	1.2 L	UPS, TDS, ELS	81Ben
	130	Kelvin	III	-1.15	1.2 L	LEED, TDS, NRA	90Cal
	180	Kelvin	III	-0.6	$\theta \approx 0.5$	c(2 × 2) structure LEED, ESDIAD, TDS, FTIR-RAS c(2×2), H <sub>2</sub> O plane highly inclined to surface normal	92Cal1
Ni(111)	100	(Kelvin)	III	-0.65	2.5 L	LEED, UPS disordered layer	87Nöb
	120	SE edge (UPS)	III	-1.1	$\theta = 0.66$	ARUPS, LEED, XPS, TDS authors propose bilayer model	89Pac



H <sub>2</sub> O, D <sub>2</sub> O/ Substrate	<i>T</i> [K]	Method	Type	$\Delta\Phi$ [eV]	at $\theta$	Comments, interpretation	Ref.
Ni(665)	150	Kelvin	III	-0.7	$\theta = 0.75$	LEED, TDS H <sub>2</sub> O decorates the steps: 11(111) terraces + 1(11 $\bar{1}$ )step	92Ben
Ni(221)	150	Kelvin	III	-1.4	$\theta = 1.1$	LEED, TDS H <sub>2</sub> O decorates the steps: 3(111) terraces + 1(11 $\bar{1}$ )step	92Ben
Ni(11 11 9)	140	Kelvin	III	-1.05		LEED, TDS H <sub>2</sub> O decorates the steps: 10.5 (111) terraces + 1(11 $\bar{1}$ )step $\mu_0 = 1.2$ D	93Mun
Ni(775)	150	Kelvin	III	-0.75	1.5 L	LEED, AES also: co-adsorption with Na	94Mun
Pd(100)	10	EELS		0.07	0.15 L	EELS, LEED	84And
Pd(110)	100	Kelvin	III	-0.73	$\theta = 0.5$	LEED, TDS	90He
Pt(110)	100	Kelvin	III	-1.0	5 L	ESDIAD, TDS	86Fus
Pt(111)	90	SE edge (UPS)	III	-1.15		UPS	89Ruc
	90	Kelvin	III	(-1.1)	5 L	LEED, AES, IRAS	97Vil
	137	Kelvin		-0.6		LEED ( $\sqrt{39} \times \sqrt{39}$ ) R16.1°	03Har
Ru(0001)	95	Diode	III	-0.6	2 L	LEED, HREELS, TDS hydrogen bonded bilayer ( $\sqrt{3} \times \sqrt{3}$ ) R30° structure	81Thi
	120	SE edge (UPS)	III	-1.2	5 L	LEED, UPS, XPS	91Pir
			III	-1.28	$\theta = 0.66$ bilayer	LEED, TDS, p( $\sqrt{3} \times \sqrt{3}$ ) $\mu_0 = 0.34$ D $\mu_0 = 0.65$ D; depolarization included with two A states for the H <sub>2</sub> O bilayer one A state for the D <sub>2</sub> O bilayer	95Hel2
	400	Kelvin		+0.20 +0.75	0.25 ML 0.5 ML	LEED, HREELS, TDS similar result for Ru(12(001)×(010))	96Koc
				+0.20 +0.77	1.6 L 6 L	similar result for Ru(12(001)×(010))	
	82	Kelvin	III	-1.3 -1.7	bilayer at 1.3 L 3.5 L	MDS, TDS	96Liv

H <sub>2</sub> O, D <sub>2</sub> O/ Substrate	<i>T</i> [K]	Method	Type	$\Delta\Phi$ [eV]	at $\theta$	Comments, interpretation	Ref.
Ru(0001) cont.	120	Kelvin	III	-1.34	2 L	TDS 2 states A <sub>1</sub> , A <sub>2</sub> for the H <sub>2</sub> O bilayer only one A state for D <sub>2</sub> O	97Hof
Zr(0001)	80	(Kelvin)	III	-1.1 -1.3	1. layer 2. layer ( $\theta=0.75$ )	LEED, TDS, NRA, FTIR-RAS	97Li2

**Table 6.** Assignments of molecular versus dissociative adsorption of water on crystalline metal surfaces;  $\Delta H$ : enthalpy difference between molecularly adsorbed water (50 kJ/mol) and dissociated water deduced from gas phase reactions (Minus sign favors dissociation). First number: complete dissociation, second number: OH + O.

Substrate	Dissociation either as minor or major pathway	Dissociation only at defect sites	No dissociation detected or indicated	$\Delta H$ [kJ/mol]
Ag(100)			84Kla, 86Din	180/120
Ag(110)			80Bow, 81Stu, 83Au, 85Ban1, 85Ban2, 86Stu, 87Ban1, 87Ban2, 87Mad, 89Wu, 90Kiz, 91Kiz	180/120
Ag(111)			84Kla	180/120
Ag(112)			84Kla	180/120
Ag(113)			83Yat	180/120
Al(100)	82Sza, 89Mem1, 93Bus, 93Sha			
Al(110)	78Ebe, 94Mil			
Al(111)	83Net, 87Cro, 88Che, 89Smi, 99Pöl			
Au(110)			87Out	220/100
Au(111)			89Kay, 93Laz, 94Coe, 96Smi, 97Ike, 98Pir	220/100
Au/Pt(335)			00Ske	220/100
Be(0001)	03Zal			
Co(11 $\bar{2}$ 0)	82Her2, 94Gre, 95Gre			-60/-20
Co(0001)	82Her2			-60/-20
Cu(100)		88Sti (at oxide impurities)	00Dvo, 80Sas, 84And, 85Spi1, 93Bro2, 97Sue	5/60
Cu(110)	03Amm, 82Spi, 85Spi2, 86Pra, 94Pol	88Sti (at oxide impurities)	83Ban1, 83Ban2, 83Mar, 84Ban, 86Stu, 89Lac	5/60
Cu(111)	79Au	88Sti (at oxide impurities)	83Ban1, 91Hin, 92Hin	5/60
Cu(113)	93Xu			5/60
Cu/Ru(0001)			91Rod	5/60
Fe(100)	01Suz, 77Dwy, 82Bar, 91Hun, 93Hun			-110/-10
Fe(110)	82Dwy			-110/-10

Substrate	Dissociation either as minor or major pathway	Dissociation only at defect sites	No dissociation detected or indicated	$\Delta H$ [kJ/mol]
Fe(111)	96Jia			-110/-10
$\gamma$ -Fe(111) film	97Rub			-110/-10
FeAl(100)	96Gle			
Ir(110)		81Wit		80/-
Nb(110)	93Col			-240/-
Ni(100)	77Nor, 84Pee, 97Kam		93Bro1	-40/-5
Ni(110)	78Fal, 79Hop, 85Oll, 86Hoc, 88Ben, 89Gri, 90Cal, 91Cal, 92Cal1, 92Cal2, 94Pir, 98Kov	82Ben (at oxygen impurities)		-40/-5
Ni(111)		92Ben, 93Mun, 94Mun, 96Rei, 98Mun	81Net, 82Mad, 85Stu, 87Mad, 87Nöb, 89Pac, 93Kuc1, 93Kuc2, 94Kuc, 95Sch	-40/-5
Ni(760)	96Kas			-40/-5
Ni(210)	83Car			-40/-5
NiAl(110)	95Gle			
Ni <sub>3</sub> (Al,Ti)(100)	95Chi1, 95Chi2, 96Chi			
Ni <sub>3</sub> (Al,Ti)(110)	95Chi1			
Ni <sub>3</sub> (Al,Ti)(111)			95Chi1, 95Chi2	
Pb(110)			93Au	
Pd(100)			84Nyb, 86Kis, 86Nyb	110/45
Pd(110)			90Bro1, 90Bro2, 90He, 91Bro, 92Xu, 95Ben	110/45
Pd(111)			91Wol, 91Zhu	110/45
Pt(100)			92Kiz, 94Gri	170/75
Pt(110)-(1×2)			86Fus, 99Che	170/75
Pt(111)		96Gri (at Si impurities)	01Jac1, 80Fis1, 80Fis2, 80Iba, 80Sex, 82Cre, 84Lan, 85Kis, 87Wag2, 88Wag1, 88Wag2, 89Ran1, 89Ran2, 91Jo, 91Lac, 91Mau, 91Sas, 92Sta, 93Sta, 94Oga, 95Bau, 95Kiz, 95Vil, 96Gil, 96Mor, 97Gle, 97Mor, 97Wan, 98Löf, 98Oga, 98Su, 99Gle, 99Nak, 99Oga	170/75
Pt(111), stepped			00Ske, 81Mil	170/75
Pt <sub>x</sub> Sn <sub>y</sub> (111)			98Pan	
Re(0001)	84Jup			-60/-
Rh(111)			80Zin, 87Wag1, 88Wag1	100/-
Rh(100)			85Heg	100/-
Ru(1000)			89Lea1, 89Lea2	60/-

Substrate	Dissociation either as minor or major pathway	Dissociation only at defect sites	No dissociation detected or indicated	$\Delta H$ [kJ/mol]
Ru(0001)	91Pir, 95Hel2	82Kre (at oxide impurities), 77Mad, 84Thi	01Lil, 01Nak, 03Den, 03Pui, 80Thi, 81Kre, 81Thi, 82Doe, 83Doe, 83Wil, 86Pol, 86Sem, 87Pol, 87Sch, 89Lea1, 90Cou, 94Shi, 95Rom, 96Sch, 97Hof, 98Ras, 99Liv	60/-
Sr/Si(111)	01Mau			
Ti(0001)	82Sto			-350/-
W(100)	67Pro, 88Mue			-150/-
W(110)	90Mue			-150/-
Y(0001)	03Bly			
Zn(0001)			84Au, 86Sen	-150/-70
Zr(0001)	00Kan, 02Kan, 03Ank, 97Li1, 97Li2		83Zwi	-430/-
C(0001)			93Cha, 95Cha1, 95Cha2, 95Phe	

**Table 7.** Desorption temperatures of water from different crystalline metal surfaces ordered with respect to their assigned adsorption geometry and desorption paths, respectively

Substrate	Multilayer	Bilayer	At steps/ defects/ disociation products	Recombi- nation	Reference
Ag(100)	170 K	-			84Kla
Ag(110)	170 K	-			86Stu, 81Stu
	140 K	-			90Kiz
	160 K	-			85Ban2, 85Ban1
	155 K	-			85Ban1, 87Mad
Ag(111)	170 K	-			84Kla
Al(100)				210 K	89Mem1*
Al(111)	155 K	160-200 K			87Cro
	160 K			320 /650 K	88Che, 99Pöl
Au(110)	185 K	190 K			87Out
Au(111)	160 K				89Kay, 93Laz
Au/Pt(335)	161 K				00Ske
C(0001)	150 K		180 K		95Cha1
Co(0001)	140 K				82Her2 <sup>1</sup>
Co(1120)	155 K	170 K		270	82Her2 <sup>1</sup>
Cu(100)	150 K				00Dvo, 93Bro2, 97Sue
	162 K				
	170 K		170 K		
Cu(110)	165 K	175 K			89Lac, 94Pol, 90Lac, 91Lac
	160 K	175 K			83Ban1
	165 K	170 K			84Ban
	170 K	175 K			86Stu
	175 K				89Cle

Substrate	Multilayer	Bilayer	At steps/ defects/ dissociation products	Recombi- nation	Reference
Cu(111)	155 K 175 K				92Hin 83Ban1
Cu/Ru(0001)		190 K			91Rod
Fe(100)	165 K	220 K		310 K	91Hun
$\gamma$ -Fe(111) film	180 K	188 K			97Rub
FeAl(110)	150 K			(300 K) <sup>2</sup>	96Gle
Ir(110)	160 K	200 K		270/300 K	81Wit
Ni(100)	170 K 174 K	182 K 185 K			97Kam 84Pee*
Stepped Ni(100)	160 K	210 K	260 K	350 K	88Ben, 92Cal1 <sup>+</sup> , 96Kas*
Stepped Ni(110)	160 K	210 K	250 K 260 K	370 K 360 K	89Gri* 78Fal
		212 K	250 K	340 K	96Kas
Ni(111)	150-155 K 153 K	170 K 165 K			82Mad, 85Stu, 87Mad, 89Pac, 93Kuc2, 95Sch
Stepped Ni(111)	160 K	175 K	225 K	260-325 K	87Nöb, 92Ben, 95Jac
Ni <sub>3</sub> (Al,Ti)(110)	160 K	190 K		500 K	00Wan
Ni <sub>3</sub> (Al,Ti)(111)	250 K				95Chi1, 95Chi2
Pb(110)					93Au
Pd(100)	167 K	175 K 170 K			84Nyb <sup>+</sup> , 84Stu
Pd(110)	160 K 155 K	195 K 167 K			90He, 90Bro1, 91Bro <sup>+</sup> , 92Xu
Pd(111)	155 K	165 K			91Wol, 91Zhu
Pt(100)	150 K 170 K	165 K			80Iba 92Kiz
Pt(111)	160 K 165 K 160 K 165 K 150 K 155 K 155 K 164 K 165 K 153 K	170 K 175 K 180 K 180 K 165 K 168 K 171/177 K 185 K 168 K	200 K 195 K 200 K		80Fis1, 91Mau, 96Gri*, 98Pan, 98Su 96Gil <sup>+</sup> 88Wag1, 97Wan* 94Oga*, 98Oga* 02Haq 00Ske 91Jo* 04Gre 02Haq
Re(0001)	140 K	150 K	180 K	250-450 K	84Jup
Rh(100)	170 K	190 K			85Heg
Rh(111)	150 K 158 K 165 K	170 K 183 K 191 K	200 K		00Gib 86Kis 80Zin
Ru(1010)	160 K 170 K	190-220 K 180-240 K			89Lea2 <sup>+</sup> 89Lea1

Substrate	Multilayer	Bilayer	At steps/ defects/ dissociation products	Recombi- nation	Reference
Ru(0001)/H <sub>2</sub> O	150 K	170/212 K	230/260 K		94Hel2, 95Hel2, 95Rom
	155 K	170/210 K			90Cou
	155 K	175/220 K			86Pol
	155 K	180/215 K			82Doe, 83Doe
	155 K	190/212 K			97Hof
	160 K	185/220 K			81Thi, 84Thi, 99Liv
	160 K	175/215 K			01Lil
	165 K	185/215 K			82Kre, 87Sch, 96Liv
	170 K	180/220 K			89Lea1
	170 K	200/220 K			87Pol
	185 K	200/230 K			77Mad
	-	185/220 K			80Thi, 86Sem
Ru(0001)/D <sub>2</sub> O	150 K	180-190 K			83Doe*, 94Hel2*, 95Hel2*
	155 K	185 K			97Hof*
	160 K	185 K			01Lil*
	165 K	185 K			87Sch*
	170 K	185 K			89Lea1*
Sn-Pt(111)	160 K	166 K			98Pan
Zr(0001)	163 K	178 K			97Li2

<sup>1</sup>deduced from temperature dependent UPS; <sup>2</sup>parantheses indicate that dissociation leads to H<sub>2</sub> desorption only  
 \* D<sub>2</sub>O; + D<sub>2</sub>O = H<sub>2</sub>O

**Table 8.** Adsorption structure of water on metal surfaces; temperature and coverages in fraction of a bilayer partly estimated from data given in Langmuir are given; D: Dimer, T: Tetramer, H: Hexamer

Substrate	Monomere	Di-/Tetra- /Hexamere	Larger cluster	Dissociation	Ref
Ag(100)			150 K		86Din
Ag(110)			160 K		89Wu
			100 K/>0.2		81Stu
Ag(111)		70 K/0.5 H	70 K/0.5		02Mor1
Al(100)			130 K/>0.05		94Gri
Al(111)	20 K/<0.05		20 K/>0.05		91Jac
			127 K/>0.5	130 K	87Cro
			90 K/>0.5	>90 K	88Che
Au(111)			120 K		98Pir
			100 K/ ~1.0		97Ike
C(0001)			85 K/>0.2		95Cha1, 95Phe
Cu(100)			90-140 K/>0.3		85Spi1
	10 K/0.1				86Nyb
	10 K/0.1				84And
Cu(110)			130-170 K/>0.1		89Lac
	90-190 K/>0.05		90 -175 K/>0.05		94Pol
			100 K/0.1		91Sas
	90-140 K/<0.5				82Spi
Cu(111)	<16 K/0.03				02Mor2
			150 K/>0.4		91Hin

Substrate	Monomere	Di-/Tetra- /Hexamere	Larger cluster	Dissociation	Ref
Fe(100)			130 K/>0.1 100 K/>0.5	130 K/<0.1 200 K/>0.5	82Bar 91Hun
Ni(100)		140 K/<0.1 D 130 K/<0.2	140 K/>0.1 130 K/>0.01		93Bro1 92Ell
Ni(110)			>110 K/<0.1		86Hoc
		150 K/>0.01 H			85Oll
	80-200 K/<0.5			>120 K	94Pir
		80-200 K/<0.5 D	80-200 K, >0.5		90Cal, 91Cal, 92Cal1, 94Gri, 94Pir, 98Kov 85Nöb, 88Ben, 91Cal, 94Pir
Pd(100)	10 K/<0.05		110 K/0.1-1 80 K/>0.1		84And, 86Nyb 84Nyb, 86Nyb 84Stu
Pd(110)	120 K/<0.1 100 K/<0.1	100 K/<0.1 T	120 K/>0.02 120 K/>0.1 100 K/>0.15 100 K/>0.1		95Ben 92Xu 90Bro1 93Bro1 90Bro2, 93Bro1
Pd(111)	<40 K/<0.01		>40 K		02Mit
Pt(100)			150 K/>0.1		80Iba
Pt(110)			100 K/>0.05 130 K/>0.1		86Fus 94Gri
Pt(111)	40 K/<0.05 85 K/<0.01 20 K/<0.1 84 K/<0.13 25-40 K/<0.18	40-100 K /<0.15 D/T 20 K/0.2-0.5 D/T	100-130 K 85 K/>0.01 >130 K/0.4 84 K/>0.13 25 K/>0.27 90-140 K/>0.1		97Gle, 99Gle 01Jac1 99Nak 94Oga, 98Oga 99Oga 80Sex, 84Lan, 87Wag1, 89Ran1, 95Bau, 96Mor, 97Mor
Re(0001)	80K/<0.07	80 K/0.07-0.3	80 K/>0.3		84Jup
Rh(111)			90 K/>0.1		87Wag1
Ru(0001)	80K/<0.02		80-200 K/>0.1		84Thi 80Thi, 81Kre, 81Thi, 82Kre, 82Thi1, 84Thi, 91Pir, 94Shi
	20 K/0.1	20 K/>0.2 T	> 70 K/>0.1		00Nak, 01Nak 00Nak, 01Nak, 02Nak 00Nak
		50 K/0.1 T	95 K/>0.01		81Thi

Substrate	Monomere	Di-/Tetra-/Hexamere	Larger cluster	Dissociation	Ref
Zn(0001)			80-120 K/>0.1	>120 K	86Sen
Zr(0001)			80 K/>0.23	80 K/<0.23	97Li2

**Table 9.** Measured superstructure periodicity of ordered 2D ice bilayers on solid surfaces (no=no long-range order observed).

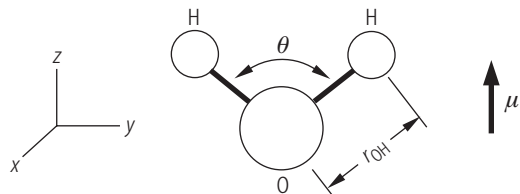
Substrate	Long range structure	Temperature	Reference
Ag(100)	no	80 K	84Kla
Ag(110)	no	80-160 K	85Ban2, 86Stu
Ag(111)	no	80 K	84Kla
	hexagonal along 112/110	155 K	79Fir
Ag(112)	no	80 K	84Kla
Al(100)	no	130 K	94Gri
Al(111)	no	80 K	83Net
Au(111)	( $\sqrt{3}\times\sqrt{3}$ )R30°	120 K	98Pir
Co(0001)	no	100 K	82Her2
Co(11 $\bar{2}$ 0)	no	100 K	82Her2
Cu(100)	no	90 K	85Spi1
Cu(110)	c(2×2)	90 K	94Pol
	c(2×2)	100-130 K	83Ban2, 84Ban, 86Stu, 89Lac
	c(2×2)	90 K	82Spi
Ir(110)	no	130 K	81Wit
Ni(110)	c(2×2)	180 K	90Cal, 92Cal1
	c(2×2)	80-150 K	85Nöb, 88Ben, 94Gri
Ni(111)	( $\sqrt{3}\times\sqrt{3}$ )R30°	80 K	81Net, 82Mad
	( $\sqrt{3}\times\sqrt{3}$ )R30°	120 K	89Pac
	( $\sqrt{3}\times\sqrt{3}$ )R30°	150 K	93Mun
Pd(100)	no	110 K	84Nyb
Pd(110)	c(2×2)	100 K	90He, 92Xu
Pd(111)	( $\sqrt{3}\times\sqrt{3}$ )R30° lace structure	100 K	04Cer <sup>c</sup>
Pt(110)	no	100 K	86Fus
Pt(111)	( $\sqrt{3}\times\sqrt{3}$ )R30°	100 K	80Fis1, 87Wag1
	( $\sqrt{37}\times\sqrt{37}$ )R25.3° and	130-140 K	97Gle <sup>a</sup> , 97Mor <sup>c</sup>
	( $\sqrt{39}\times\sqrt{39}$ )R16.1° domains <sup>a</sup>	130-135 K	02Haq, 03Har, 97Glea
	hexagonal	160 K	92Sta, 93Sta, 95Mat, 97Mor
Re(0001)	( $\sqrt{3}\times\sqrt{3}$ )R30°	80 K	84Jup
	(2×2)	150 K	84Jup
Rh(111)	( $\sqrt{3}\times\sqrt{3}$ )R30°	80-100 K	80Zin, 87Wag1, 88Wag1
	( $\sqrt{3}\times\sqrt{3}$ )R30°+superstructure	80 K	00Giba
Ru(0001)	( $\sqrt{3}\times\sqrt{3}$ )R30°H <sub>2</sub> O	95 K	81Thi
	( $\sqrt{3}\times\sqrt{3}$ )R30°H <sub>2</sub> O <sup>c</sup>	80-175 K	82Doe, 83Wil, 91Pir
	( $\sqrt{3}\times\sqrt{3}$ )R30°D <sub>2</sub> O	100-150 K	03Pui, 94Hel2, 95Hel1,
	H <sub>2</sub> O-domains: $\begin{pmatrix} 1 & 2 \\ 0 & N \end{pmatrix}$ phases (N=13 / 19-20)		95Hel2 <sup>b</sup>



Substrate	Long range structure	Temperature	Reference
Zr(0001)	no	80 K	97Li2

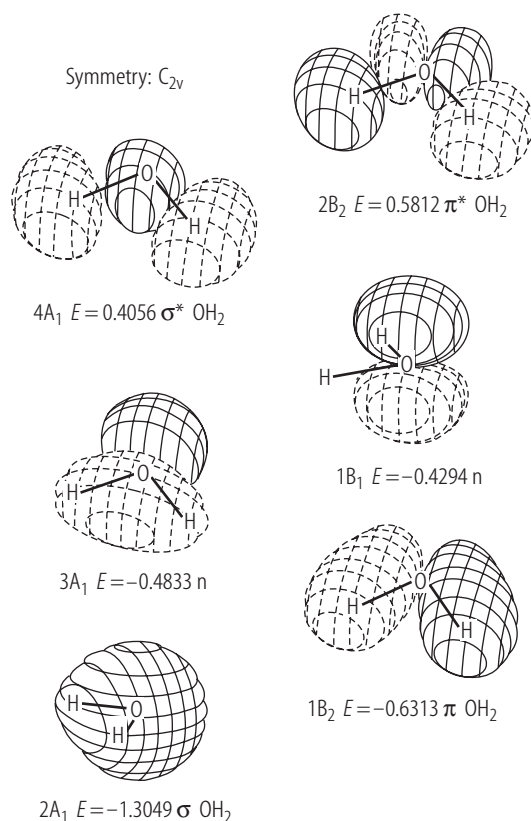
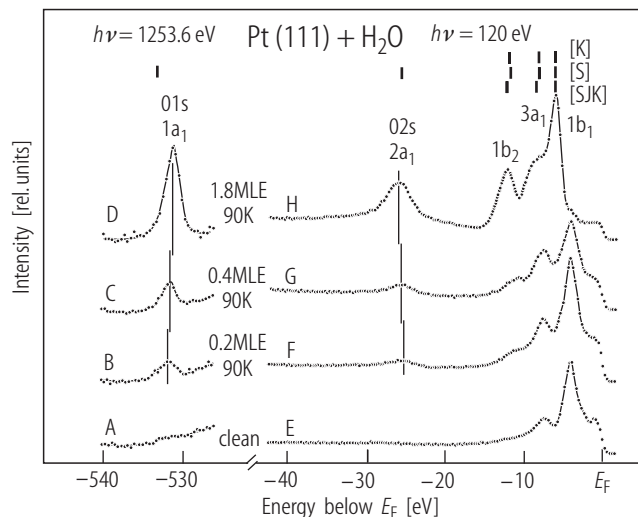
a. Detected with He atom scattering, b. Detected with both He atom scattering and LEED, c. detected by STM

### 2.7.0.5 Figures for 3.8.1

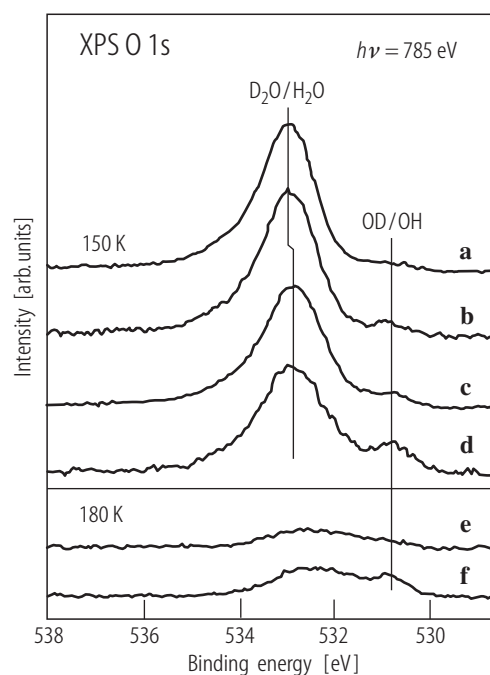


**Fig. 1.** Schematic geometric model of H<sub>2</sub>O [87Thi].

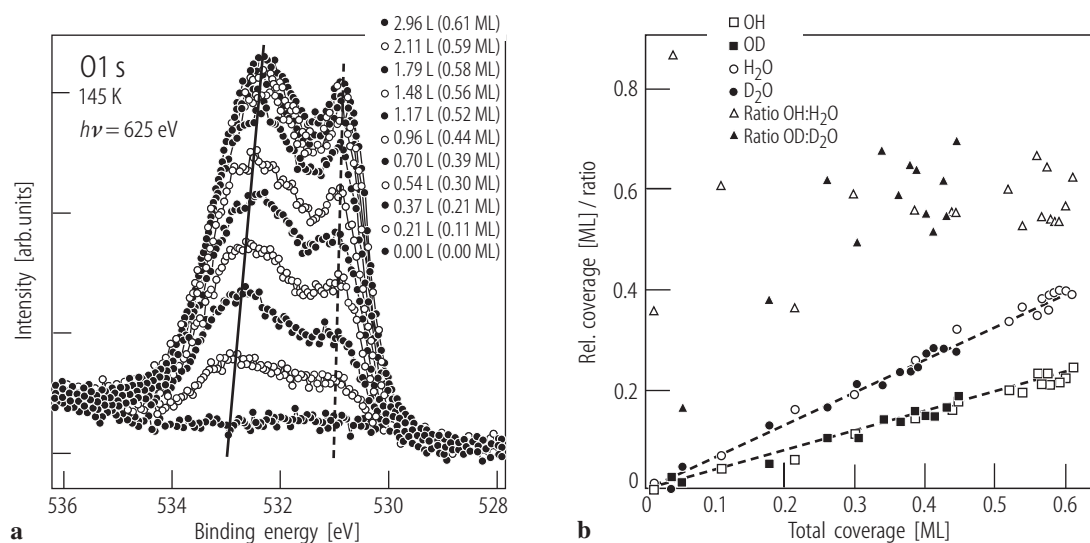
**Fig. 3.** Photoelectron spectra for the O1s, O2s and the valence band region of H<sub>2</sub>O at different H<sub>2</sub>O coverages on Pt(111); coverages are indicated in monolayer equivalent: 1 MLE =  $1.5 \times 10^{15} \text{ cm}^{-2}$ . In addition, the peak energies related to the 1b<sub>1</sub> peak are shown as lines for condensed water (SJK,  $h\nu = 40 \text{ eV}$  [80Sch]) and water gas (S,  $h\nu = 1253.6 \text{ eV}$  [69Sie]; K,  $h\nu = 21.2 \text{ eV}$  [81Kim]) [89Ran1].



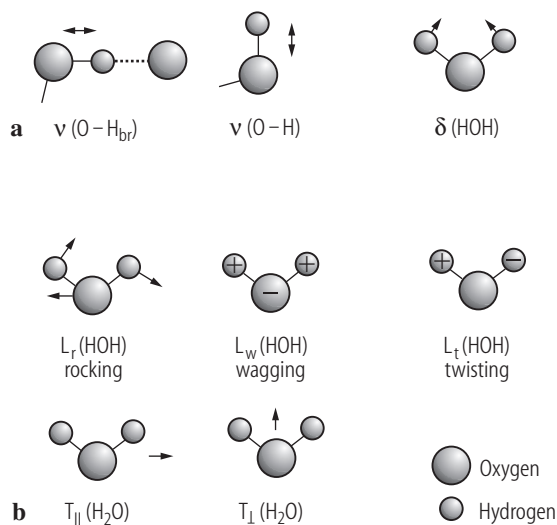
**Fig. 2.** Delocalized molecular orbitals of H<sub>2</sub>O [73Jor].



**Fig. 4.** O 1s photoelectron spectra for water mono-layers on Ru(0001) adsorbed at 150 K (a-d) and after an additional water exposure of  $10^{13} \text{ mole-cules cm}^{-2} \text{ s}^{-1}$  at 180 K (e-f): D<sub>2</sub>O/OD (a, b, e) H<sub>2</sub>O/OH (c, d, f). Spectra b and d were taken after a X-ray irradiation 60 times larger than for spectra a and b [04And].

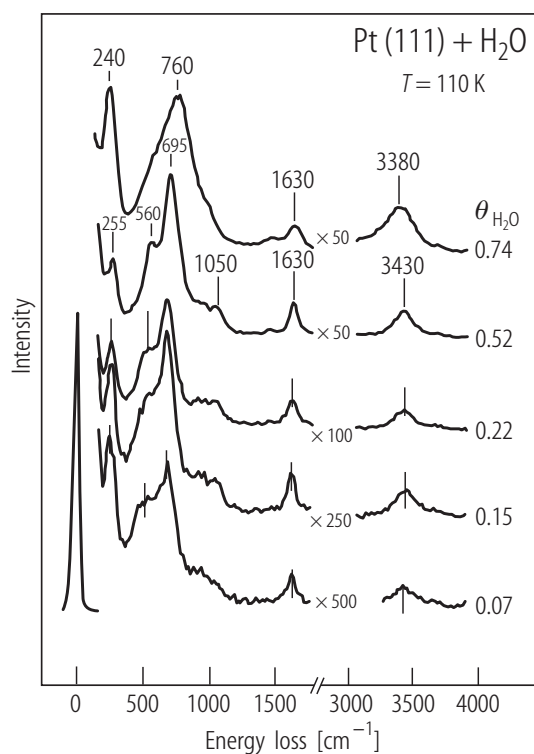


**Fig. 5.** a) O 1s spectra during H<sub>2</sub>O adsorption on Ru(0001) at 145 K and  $1.6 \times 10^{-9}$  mbar with a collection time of 140 s per spectrum, corresponding coverages are indicated. b) coverage dependence of OH (OD) and H<sub>2</sub>O (D<sub>2</sub>O) peak intensities ( $\circ$ ,  $\bullet$ ,  $\square$ ,  $\blacksquare$ ) and their ratios ( $\Delta$ ,  $\blacktriangle$ ) at 145 K [04Wei].



**Fig. 6.** Sketch of a) intramolecular and b) extra-molecular vibrational modes for H<sub>2</sub>O [01Jac1].

**Fig. 7.** HREEL spectra of H<sub>2</sub>O on a Pt(111) surface for increasing coverages as indicated [95Bau].



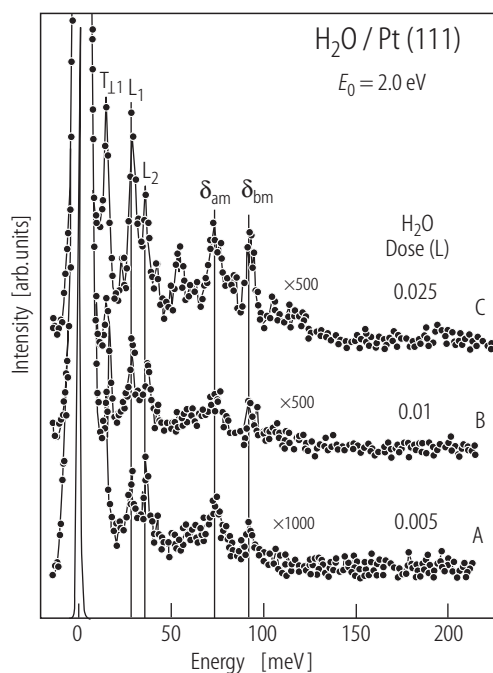


**Fig. 8.** HREEL spectra for small H<sub>2</sub>O exposures on Pt(111); the assignment of the peaks is indicated and described within the text [01Jac1].

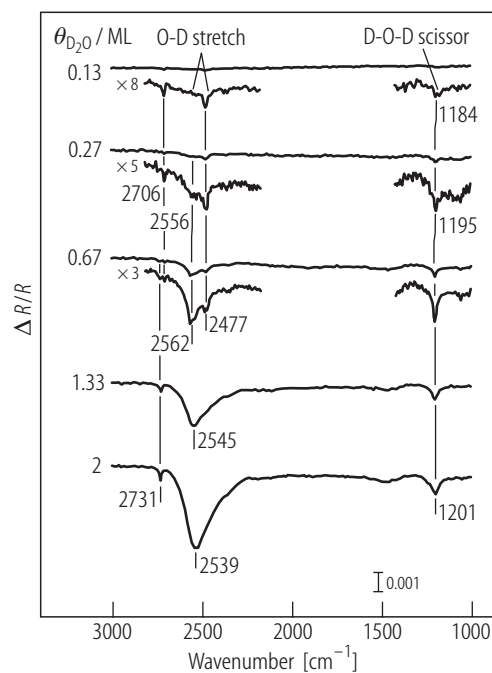


**Fig. 9** IRAS spectra of D<sub>2</sub>O on Pt(111) adsorbed at 84 K at different coverages as indicated on the left. The origin of the vibrational lines is marked. O-D-stretch corresponds to the second mode displayed in Fig. 6a and D-O-D-scissor to the third mode in Fig. 6a. Note the two lines of the O-D-stretch mode which are assigned to D<sub>2</sub>O monomers and D<sub>2</sub>O bound in clusters (courtesy of H. Ogasawara) [94Oga].

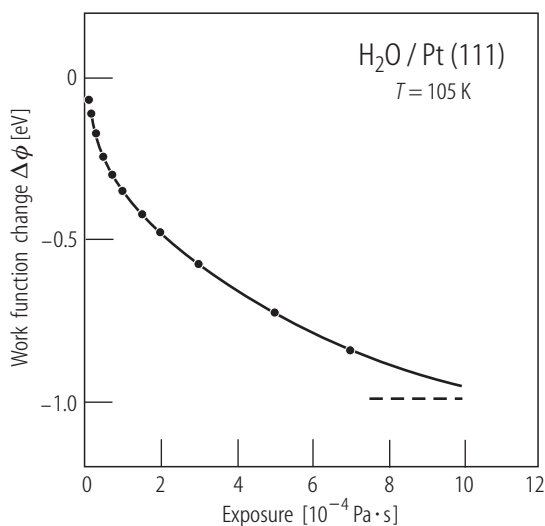


**Fig. 10.** Work function change versus H<sub>2</sub>O exposure for H<sub>2</sub>O on Pt(111) at 105 K [85Kis]

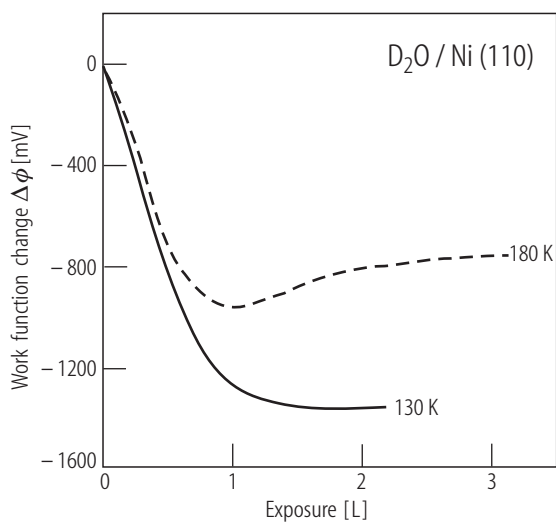


**Fig. 11.** Work function change versus D<sub>2</sub>O exposure for D<sub>2</sub>O on Ni(110) at 180 K and 130 K [90Cal]

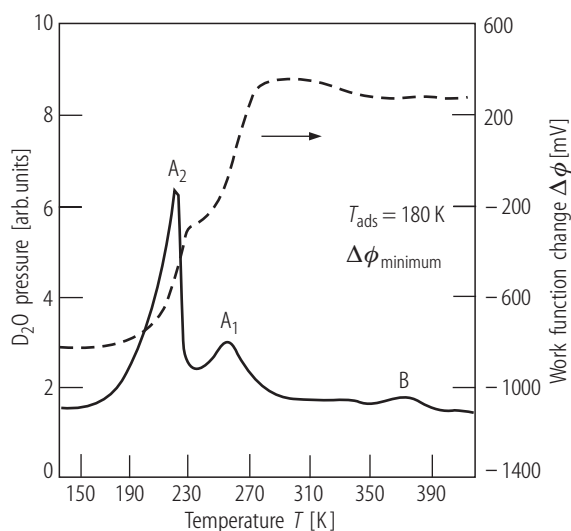


**Fig. 12.** Thermal desorption spectra (full line) and work function changes (broken line) for D<sub>2</sub>O dosed onto Ni(110) at 180 K for an exposure corresponding to the minimum of  $\Delta\phi$  in Fig. 11 [90Cal].

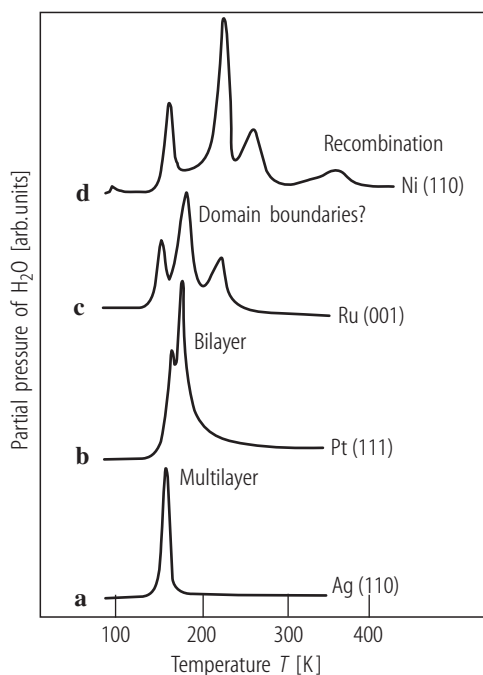


**Fig. 13.** TPD spectra of H<sub>2</sub>O from different substrates as indicated; coverage: Ag(111) 3.0 L, Pt(111) 3.8 L, Ru(0001) 2.0 L, Ni(110) not known. The origin of the different desorption peaks is marked (courtesy of P. A. Thiel) [87Thi].

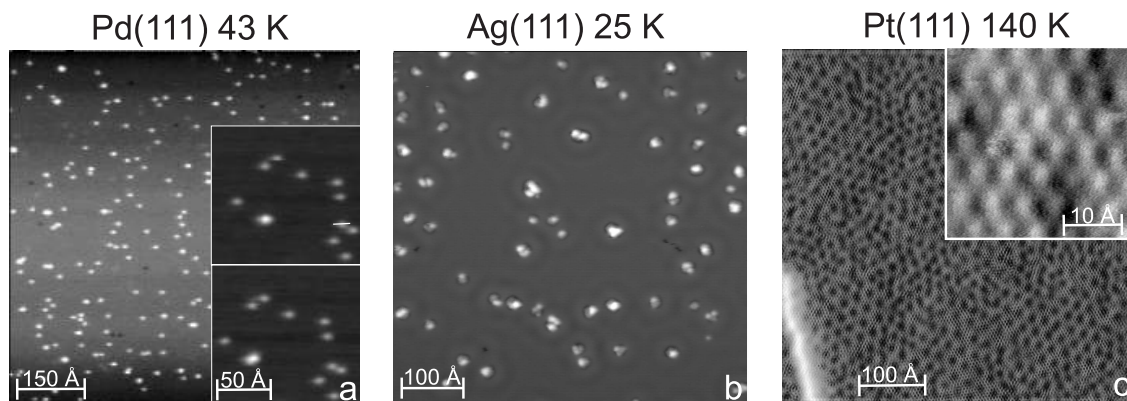


**Fig. 14.** STM images of H<sub>2</sub>O adsorbed on different surfaces at different temperatures as indicated. (a) H<sub>2</sub>O monomers on Pd(111); inset: two consecutive images showing the diffusion of individual monomers e.g. of the monomer marked by a white line in the upper image (courtesy of E. Fomin and M. Salmeron) [02Mit]. (b) Small H<sub>2</sub>O clusters of different size (1-10 atoms) on Ag(111), coverage: 0.1 molecules/nm<sup>2</sup> (courtesy of K. Morgenstern) [02Mor1, 02Mor2]. (c) Complete H<sub>2</sub>O bilayer on Pt(111); the visible network is due to a superstructure explained by the misfit between the H<sub>2</sub>O bilayer and Pt(111) (phase I); inset: larger resolution image showing the arrangement of the H<sub>2</sub>O molecules within the bilayer [97Mor].

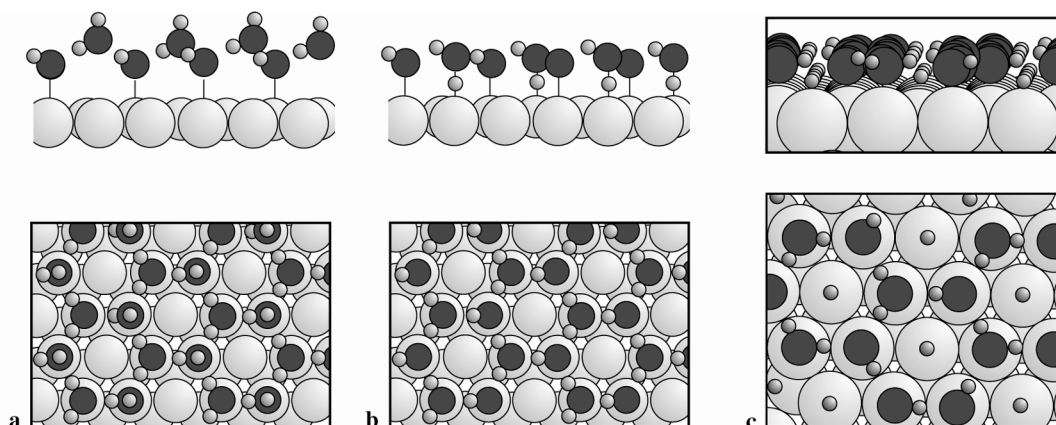


**Fig. 15.** Structural models of the ice bilayer on close-packed metal surfaces: upper row: side view, lower row: top view. (a) Usually assumed  $\sqrt{3}\times\sqrt{3}$  superstructure of a perfect H<sub>2</sub>O bilayer with only oxygen atoms binding to the metal surface (courtesy of H. Ogasawara). (b) Model for the H<sub>2</sub>O bilayer on Pt(111) with oxygen and hydrogen atoms binding to the metal surface; the model is based on the analysis of X-ray-absorption, X-ray emission and X-ray photoelectron spectroscopy experiments (courtesy of H. Ogasawara) [02Oga]. (c) Model for the H<sub>2</sub>O bilayer on Ru(0001) involving partial dissociation of H<sub>2</sub>O into OH and H; the model is concluded from ab initio calculations based on density functional theory (courtesy of P. Feibelman) [02Fei].

## 3.8.1.7 References for 3.8.1

- 67Pro Propst, F.M., Piper, T.C.: *J. Vac. Sci. Technol.* **4** (1967) 53.
- 69Eis Eisenberg, D., Kauzmann, W.: *The structure and properties of water*, New York: Oxford University Press, 1969.
- 69Sie Siegbahn, K., Nordling, C., Johansson, G., Hedman, J., Hedén, J., Hamrin, K., Gelius, U., Bergmark, T., Werme, I.O., Manne, R., Baer, Y.: *ESCA applied to free molecules*, Amsterdam: North Holland, 1969.
- 71Cot Cotton, F.A.: *Chemical application of group theory*, 2nd ed., New York: Wiley-Interscience, 1971.
- 73Jor Jorgensen, W.L., Salem, L.: *The organic chemist's book of orbitals*, New York, San Francisco, London: Academic Press, 1973.
- 74Rab Rabalais, J.W., Debies, T.P., Berkosky, J.L., Huang, J.T.J., Ellison, F.O.: *J. Chem. Phys.* **61** (1974) 516.
- 75Che Chesters, M.A., Somorjai, G.A.: *Surf. Sci.* **52** (1975) 21.
- 76Wha Schuster, P., Zundel, G., Sandorfy, C.: Dynamics, thermodynamics and special systems, in: *The Hydrogen Bond*, Vol. 3, Whalley, E. (ed.), Amsterdam: North-Holland, 1976.
- 77Con Connor, J.A., Considine, M., Hillier, I.H.: *J. Electron Spectrosc. Relat. Phenom.* **12** (1977) 143.
- 77Dwy Dwyer, D.J., Simmons, G.W., Wei, R.P.: *Surf. Sci.* **64** (1977) 617.
- 77Mad Madey, T.E., Yates, J.T.: *Chem. Phys. Lett.* **51** (1977) 77.
- 77Nor Norton, P.R., Tapping, R.L., Goodale, J.W.: *Surf. Sci.* **65** (1977) 13.
- 78Ebe Eberhardt, W., Kunz, C.: *Surf. Sci.* **75** (1978) 709.
- 78Fal Falconer, J.L., Madix, R.J.: *J. Catal.* **51** (1978) 47.
- 79Au Au, C.T., Breza, J., Roberts, M.W.: *Chem. Phys. Lett.* **66** (1979) 340.
- 79Fir Firment, L.E., Somorjai, G.A.: *Surf. Sci.* **84** (1979) 275.
- 79Hop Hopster, H., Brundle, C.R.: *J. Vac. Sci. Technol.* **16** (1979) 548.
- 80Au Au, C.T., Roberts, M.W.: *Chem. Phys. Lett.* **74** (1980) 472.
- 80Bow Bowker, M., Barteau, M.A., Madix, R.J.: *Surf. Sci.* **92** (1980) 528.
- 80Fis1 Fisher, G.B., Gland, J.L.: *Surf. Sci.* **94** (1980) 446.
- 80Fis2 Fisher, G.B., Sexton, B.A.: *Phys. Rev. Lett.* **44** (1980) 683.
- 80Iba Ibach, H., Lehwald, S.: *Surf. Sci.* **91** (1980) 187.
- 80Sas Sass, J.K., Richardson, N.V., Neff, H., Roe, D.K.: *Chem. Phys. Lett.* **73** (1980) 209.
- 80Sch Schmeisser, D., Jacobi, K., Kolb, D., in: *Proc. 4th Int. Conf. on Solid Surfaces and 3rd European Conf. on Surface Science*, Les Couches Minces 201, Le Vide, Suppl., Vol. I, 1980, p. 256.
- 80Sex Sexton, B.: *Surf. Sci.* **94** (1980) 435.
- 80Thi Thiel, P.A., Hoffmann, F.M., Weinberg, W.H.: *Vide Couches Minces* **201** (1980) 307.
- 80Zin Zinck, J.J., Weinberg, W.H.: *J. Vac. Sci. Technol.* **17** (1980) 188.
- 81Ben Benndorf, C., Nöbl, C., Rüsenberg, M., Thieme, F.: *Surf. Sci.* **111** (1981) 87.
- 81Kim Kimura, K., Katsumata, S., Achiba, Y., Yamazaki, T., Iwata, S.: *Handbook of HeI photoelectron spectra of fundamental organic molecules*, Tokyo: Japan Science Societies Press, 1981.
- 81Kre Kretzschmar, K., Sass, J.K., Hofmann, P., Ortega, A., Bradshaw, A.M., Holloway, S.: *Chem. Phys. Lett.* **78** (1981) 410.
- 81Mil Miller, J.N., Lindau, I., Spicer, W.E.: *Surf. Sci.* **111** (1981) 595.
- 81Net Netzer, F.P., Madey, T.E.: *Phys. Rev. Lett.* **47** (1981) 928.
- 81Stu Stuve, E.M., Madix, R.J., Sexton, B.: *Surf. Sci.* **111** (1981) 11.
- 81Thi Thiel, P.A., Hoffmann, F.M., Weinberg, W.H.: *J. Chem. Phys.* **75** (1981) 5556.
- 81Wit Wittrig, T.S., Ibbotson, D.E., Weinberg, W.H.: *Surf. Sci.* **102** (1981) 506.
- 82Bar Baró, A.M., Erley, W.: *J. Vac. Sci. Technol.* **20** (1982) 580.
- 82Ben Benndorf, C., Nöbl, C., Thieme, F.: *Surf. Sci.* **121** (1982) 249.
- 82Cre Creighton, J.R., White, J.M.: *Chem. Phys. Lett.* **92** (1982) 435.

- 82Doe Doering, D.L., Madey, T.E.: Surf. Sci. **132** (1982) 305.  
 82Dwy Dwyer, D.J., Kelemen, S.R., Kaldor, A.: J. Chem. Phys. **76** (1982) 1832.  
 82Her1 Heras, J.M., Albano, E.V.: Z. Phys. Chem. N. F. **129** (1982) 11.  
 82Her2 Heras, J.M., Papp, H., Spiess, W.: Surf. Sci. **117** (1982) 590.  
 82Iba Ibach, H., Mills, D.L.: Electron energy loss spectroscopy and surface vibrations, New York, London, Paris, San Diego, San Francisco, Sao Paulo, Sydney, Tokyo, Toronto: Academic Press, 1982.  
 82Kre Kretzschmar, K., Sass, J.K., Bradshaw, A.M., Holloway, S.: Surf. Sci. **115** (1982) 183.  
 82Mad Madey, T.E., Netzer, F.P.: Surf. Sci. **117** (1982) 549.  
 82Spi Spitzer, A., Lüth, H.: Surf. Sci. **120** (1982) 376.  
 82Sto Stockbauer, R.L., Hanson, D.M., Flodström, S.A., Madey, T.E.: J. Vac. Sci. Technol. **20** (1982) 562.  
 82Sza Szalkowski, F.J.: J. Chem. Phys. **77** (1982) 5224.  
 82Thi1 Thiel, P.A., Hoffmann, F.M., Weinberg, W.H.: Proc. 2nd. Int. Conf. on Vibrations and Surfaces, 1982, p. 201.  
 82Thi2 Thiel, P.A., Hoffmann, F.M., Weinberg, W.H.: Phys. Rev. Lett. **49** (1982) 501.  
 83Au Au, C.T., Singh-Boparai, S., Roberts, M.W., Joyner, R.W.: J. Chem. Society Faraday Trans. **179** (1983) 1779.  
 83Ban1 Bange, K., Döhl, R., Grider, D.E., Sass, J.K.: Vacuum **33** (1983) 757.  
 83Ban2 Bange, K., Grider, D.E., Sass, J.K.: Surf. Sci. **126** (1983) 437.  
 83Car Carley, A.F., Rassias, S., Roberts, M.W.: Surf. Sci. **135** (1983) 35.  
 83Doe Doering, D.L., Semancik, S., Madey, T.E.: Surf. Sci. **133** (1983) 49.  
 83Mar Mariani, C., Horn, K.: Surf. Sci. **126** (1983) 279.  
 83Net Netzer, F.P., Madey, T.E.: Surf. Sci. **127** (1983) L102.  
 83Phu Phu, S.U., Bardolle, J., Bujor, M.: Surf. Sci. **129** (1983) 219.  
 83Wil Williams, E.D., Doering, D.L.: J. Vac. Sci. Technol. A **1** (1983) 1188.  
 83Yat Yates, J.T., Ceyer, S.T.: J. Electroanal. Chem. **150** (1983) 17.  
 83Zwi Zwicker, G., Jacobi, K.: Surf. Sci. **131** (1983) 179.  
 84And Andersson, S., Nyberg, C., Tengstal, C.G.: Chem. Phys. Lett. **104** (1984) 305.  
 84Au Au, C.T., Roberts, M.W.: Proc. R. Soc. (London) A **396** (1984) 165.  
 84Ban Bange, K., Grider, D.E., Madey, T.E., Sass, J.K.: Surf. Sci. **136** (1984) 38.  
 84Bar Barteau, M.A., Madix, R.J.: Surf. Sci. **140** (1984) 108.  
 84Jup Jupille, J., Pareja, P., Fusy, J.: Surf. Sci. **139** (1984) 505.  
 84Kla Klaua, M., Madey, T.E.: Surf. Sci. (Lett.) **136** (1984) L52.  
 84Lan Langenbach, E., Spitzer, A., Lüth, H.: Surf. Sci. **147** (1984) 179.  
 84Ny Nyberg, C., Tengstal, C.G.: J. Chem. Phys. **80** (1984) 3463.  
 84Pee Peebles, D.E., White, J.M.: Surf. Sci. **144** (1984) 512.  
 84Stu Stuve, E.M., Jorgensen, S.W., Madix, R.J.: Surf. Sci. **146** (1984) 179.  
 84Thi Thiel, P.A., DePaola, R.A., Hoffmann, F.M.: J. Chem. Phys. **80** (1984) 5326.  
 85Ban1 Bange, K., Madey, T.E., Sass, J.K.: Surf. Sci. **162** (1985) 252.  
 85Ban2 Bange, K., Madey, T.E., Sass, J.K.: Surf. Sci. **152/153** (1985) 550.  
 85Bau Bauschlicher, C.W.: J. Chem. Phys. **83** (1985) 3129.  
 85Gre Greenlief, C.M., Hegde, R.I., White, J.M.: J. Phys. Chem. **89** (1985) 5681.  
 85Heg Hegde, R.I., White, J.M.: Surf. Sci. **157** (1985) 17.  
 85Kis Kiskinova, M., Pirug, G., Bonzel, H.P.: Surf. Sci. **150** (1985) 319.  
 85Nöb Nöbl, C., Benndorf, C., Madey, T.E.: Surf. Sci. **157** (1985) 29.  
 85Oll Ollé, L., Salmeron, M., Baró, A.M.: J. Vac. Sci. Technol. A **3** (1985) 1866.  
 85Spi1 Spitzer, A., Ritz, A., Lüth, H.: Surf. Sci. **152/153** (1985) 543.  
 85Spi2 Spitzer, A., Lüth, H.: Surf. Sci. **160** (1985) 353.  
 85Stu Stulen, R.H., Thiel, P.A.: Surf. Sci. **157** (1985) 99.  
 86Din Ding, X., Garfunkel, E., Dong, G., Yang, S., Hou, X., Wang, X.: J. Vac. Sci. Technol. A **4** (1986) 1468.  
 86Fus Fusy, J., Ducros, R.: Surf. Sci. **176** (1986) 157.

- 86Hoc Hock, M., Seip, U., Bassignana, I., Wagemann, K., Küppers, J.: *Surf. Sci. (Lett.)* **177** (1986) L978.
- 86Kis Kiss, J., Solymosi, F.: *Surf. Sci.* **177** (1986) 191.
- 86Nyb Nyberg, C., Tengstal, C.G., Uvdal, P., Andersson, S.: *J. Electron Spectrosc. Relat. Phenom.* **38** (1986) 299.
- 86Pol Polta, J.A., Flynn, D.K., Thiel, P.A.: *J. Catal.* **99** (1986) 88.
- 86Pra Prabhakaran, K., Sen, P., Rao, C.N.R.: *Surf. Sci.* **169** (1986) L301.
- 86Sem Semancik, S., Doering, D.L., Madey, T.E.: *Surf. Sci.* **176** (1986) 165.
- 86Sen Sen, P., Rao, C.N.R.: *Surf. Sci.* **172** (1986) 269.
- 86Stu Stuve, E.M., Bange, K., Sass, J.K.: *Trends Interfacial Electrochem., NATO ASI Ser., Ser.C* **179** (1986) 255.
- 87Ban1 Bange, K., Madey, T.E., Sass, J.K., Stuve, E.M.: *Surf. Sci.* **183** (1987) 334.
- 87Ban2 Bange, K., Straehler, B., Sass, J.K., Parsons, R.: *J. Electroanal. Chem.* **229** (1987) 87.
- 87Bon Bonzel, H.P., Pirug, G., Muller, J.E.: *Phys. Rev. Lett.* **58** (1987) 2138.
- 87Cro Crowell, J.E., Chen, J.G., Hercules, D.M., Yates, J.T.: *J. Chem. Phys.* **86** (1987) 5804.
- 87Mad Madey, T.E., Benndorf, C., Semancik, S.: *Springer Ser. Surf. Sci.* **8** (1987) 175.
- 87Nöb Nöbl, C., Benndorf, C.: *Surf. Sci.* **182** (1987) 499.
- 87Out Outka, D.A., Madix, R.J.: *J. Am. Chem. Soc.* **109** (1987) 1708.
- 87Pol Polta, J.A., Schmitz, P.J., Thiel, P.A.: *Langmuir* **3** (1987) 1178.
- 87Sch Schmitz, P.J., Polta, J.A., Chang, S.-L., Thiel, P.A.: *Surf. Sci.* **186** (1987) 219.
- 87Thi Thiel, P.A., Madey, T.E.: *Surf. Sci. Rep.* **7** (1987) 211.
- 87Wag1 Wagner, F.T., Moylan, T.E.: *Surf. Sci.* **191** (1987) 121.
- 87Wag2 Wagner, F.T., Moylan, T.E.: *Surf. Sci.* **182** (1987) 125.
- 88Ben Benndorf, C., Madey, T.E.: *Surf. Sci.* **194** (1988) 63.
- 88Che Chen, J.G., Basu, P., Ng, L., Yates, J.T.: *Surf. Sci.* **194** (1988) 397.
- 88Her Heras, C.A., Viscido, L.: *Catal. Rev. Sci.-Eng.* **30** (1988) 281.
- 88Mue Mueller, D.R., Shih, A., Roman, E., Madey, T.E., Kurtz, R.L., Stockbauer, R.L.: *J. Vac. Sci. Technol. A* **6** (1988) 1067.
- 88Sti Stickney, J.L., Ehlers, C.B., Gregory, B.W.: *ACS Symp. Ser.* **378** (1988) 99.
- 88Wag1 Wagner, F.T., Moylan, T.E., Schmieg, S.J.: *Surf. Sci.* **195** (1988) 403.
- 88Wag2 Wagner, F.T., Moylan, T.E.: *Surf. Sci.* **206** (1988) 187.
- 89Cle Clendening, W.D., Rodriguez, J.A., Campbell, J.M., Campbell, C.T.: *Surf. Sci.* **216** (1989) 429.
- 89Gri Griffiths, K., Memmert, U., Callen, B.W., Norton, P.R.: *J. Vac. Sci. Technol. A* **7** (1989) 2001.
- 89Kay Kay, B.D., Lykke, K.R., Creighton, J.R., Ward, S.J.: *J. Chem. Phys.* **91** (1989) 5120.
- 89Lac Lackey, D., Schott, J., Straehler, B., Sass, J.K.: *J. Chem. Phys.* **91** (1989) 1365.
- 89Lea1 Leavitt, P.K., Schmitz, P.J., Dyer, J.S., Polta, J.A., Thiel, P.A.: *Langmuir* **5** (1989) 679.
- 89Lea2 Leavitt, P.K., Davis, J.L., Dyer, J.S., Thiel, P.A.: *Surf. Sci.* **218** (1989) 346.
- 89Mem1 Memmert, U., Bushby, S.J., Norton, P.R.: *Surf. Sci.* **219** (1989) 327.
- 89Mem2 Memmert, U., He, J.-W., Griffiths, K., Lennard, W.N., Norton, P.R., Richardson, N.V., Jackman, T.E., Unertl, W.N.: *J. Vac. Sci. Technol. A* **7** (1989) 2152.
- 89Pac Pache, T., Steinrück, H.-P., Huber, W., Menzel, D.: *Surf. Sci.* **224** (1989) 195.
- 89Ran1 Ranke, W.: *Surf. Sci.* **209** (1989) 57.
- 89Ran2 Ranke, W., Kuhr, H.J.: *Phys. Rev. B Condens. Matter* **39** (1989) 1595.
- 89Ruc Ruckman, M.W., Jiang, L.Q., Strongin, M.: *Surf. Sci.* **221** (1989) 144.
- 89Smi Smith, P.B., Bernasek, S.L.: *J. Electron Spectrosc. Relat. Phenom.* **49** (1989) 149.
- 89Wu Wu, K.J., Peterson, L.D., Elliot, G.S., Kevan, S.D.: *J. Chem. Phys.* **91** (1989) 7964.
- 90Bla Blass, P.M., Zhou, X.L., White, J.M.: *J. Chem. Phys.* **94** (1990) 3054.
- 90Bro1 Brosseau, R., Ellis, T.H., Morin, M.: *J. Vac. Sci. Technol. A* **8** (1990) 2454.
- 90Bro2 Brosseau, R., Ellis, T.H., Morin, M., Wang, H.: *J. Electron Spectrosc. Relat. Phenom.* **54-55** (1990) 659.
- 90Cal Callen, B.W., Griffiths, K., Memmert, U., Harrington, D.A., Bushby, S.J., Norton, P.R.: *Surf. Sci.* **230** (1990) 159.



- 90Cou Coulman, D., Puschmann, A., Höfer, U., Steinrück, H.-P., Wurth, W., Feulner, P., Menzel, D.: J. Chem. Phys. **93** (1990) 58.
- 90Fus Fusy, J., Ducros, R.: Surf. Sci. **237** (1990) 53.
- 90He He, J.-W., Norton, P.R.: Surf. Sci. **238** (1990) 95.
- 90Kiz Kizhakevariam, N., Döhl-Oelze, R., Stuve, E.M.: J. Phys. Chem. **94** (1990) 5934.
- 90Lac Lackey, D., Schott, J., Sass, J.K.: J. Electron Spectrosc. Relat. Phenom. **54-55** (1990) 649.
- 90Mue Mueller, D.R., Kurtz, R.L., Stockbauer, R.L., Madey, T.E., Shih, A.: Surf. Sci. **237** (1990) 72.
- 90Sch Schott, J., Lackey, D., Sass, J.K.: Surf. Sci. **238** (1990) L478.
- 91Bor Bornemann, T., Steinrück, H.-P., Huber, W., Eberle, K., Glanz, M., Menzel, D.: Surf. Sci. **254** (1991) 105.
- 91Bro Brosseau, R., Ellis, T.H., Wang, H.: Chem. Phys. Lett. **177** (1991) 118.
- 91Cal Callen, B.W., Griffiths, K., Norton, P.R.: Phys. Rev. Lett. **66** (1991) 1634.
- 91Hin Hinch, B.J., Dubois, L.H.: Chem. Phys. Lett. **181** (1991) 10.
- 91Hun Hung, W.-H., Schwartz, J., Bernasek, S.L.: Surf. Sci. **248** (1991) 332.
- 91Jac Jacobi, K., Bertolo, M., Geng, P., Hansen, W., Schreiner, J., Astaldi, C.: Surf. Sci. **245** (1991) 72.
- 91Jo Jo, S.K., Kiss, J., Polanco, J.A., White, J.M.: Surf. Sci. **253** (1991) 233.
- 91Kiz Kizhakevariam, N., Stuve, E.M., Döhl-Oelze, R.: J. Chem. Phys. **94** (1991) 670.
- 91Lac Lackey, D., Schott, J., Sass, J.K., Woo, S.I., Wagner, F.T.: Chem. Phys. Lett. **184** (1991) 277.
- 91Mau Maurice, V., Takeuchi, K., Salmeron, M., Somorjai, G.A.: Surf. Sci. **250** (1991) 99.
- 91Pir Pirug, G., Ritke, C., Bonzel, H.P.: Surf. Sci. **241** (1991) 289.
- 91Rod Rodriguez, J.A., Campbell, R.A., Corneille, J.S., Goodman, D.W.: Chem. Phys. Lett. **180** (1991) 139.
- 91Sas Sass, J.K., Lackey, D., Schott, J.: Electrochim. Acta **36** (1991) 1883.
- 91Wol Wolf, M., Nettesheim, S., White, J.M., Hasselbrink, E., Ertl, G.: J. Chem. Phys. **94** (1991) 4609.
- 91Zhu Zhu, X.-Y., White, J.M., Wolf, M., Hasselbrink, E., Ertl, G.: J. Chem. Phys. **95** (1991) 8393.
- 92Ben Benndorf, C., Mundt, C.: J. Vac. Sci. Technol. A **10** (1992) 3026.
- 92Call Callen, B.W., Griffiths, K., Kasza, R.V., Jensen, M.B., Thiel, P.A., Norton, P.R.: J. Chem. Phys. **97** (1992) 3760.
- 92Cal2 Callen, B.W., Griffiths, K., Norton, P.R., Harrington, D.A.: J. Phys. Chem. **96** (1992) 10905.
- 92Chu Chu, X.L., Schmidt, L.D.: Surf. Sci. **268** (1992) 325.
- 92Ell Ellis, T.H., Kruus, E.J., Wang, H.: Surf. Sci. **273** (1992) 73.
- 92Hin Hinch, B.J., Dubois, L.H.: J. Chem. Phys. **96** (1992) 3262.
- 92Kiz Kizhakevariam, N., Stuve, E.M.: Surf. Sci. **275** (1992) 223.
- 92Sta Starke, U., Heinz, K., Materer, N., Wander, A., Michl, M., Döll, R., Van Hove, M.A., Somorjai, G.A.: J. Vac. Sci. Technol. A **10** (1992) 2521.
- 92Xu Xu, M., Yang, P., Yang, W., Pang, S.: Vacuum **43** (1992) 1128.
- 93Au Au, C.T., Carley, A.F., Pashuski, A., Read, S., Roberts, M.W., Zeini-Isfahan, A.: Springer Ser. Surf. Sci. **33** (1993) 241.
- 93Bro1 Brosseau, R., Brustein, M.R., Ellis, T.H.: Surf. Sci. **280** (1993) 23.
- 93Bro2 Brosseau, R., Brustein, M.R., Ellis, T.H.: Surf. Sci. **294** (1993) 243.
- 93Bus Bushby, S.J., Callen, B.W., Griffiths, K., Esposto, F.J., Timsit, R.S., Norton, P.R.: Surf. Sci. (Lett.) **298** (1993) L181.
- 93Cha Chakarov, D.V., Österlund, L., Kasemo, B.: J. Electron. Spectrosc. Relat. Phenom. **279** (1993) 64.
- 93Chu Chu, X., Chan, V., Schmidt, L.D.: Mater. Res. Soc. Symp. Proc. **312** (1993) 225.
- 93Col Colera, I., de Segovia, J.L., Wincott, P.L., Casanova, R., Thornton, G.: Surf. Sci. **292** (1993) 61.
- 93Hun Hung, W.-H., Schwartz, J., Bernasek, S.L.: Surf. Sci. **294** (1993) 21.
- 93Kuc1 Kuch, W., Schulze, M., Schnurnberger, W., Bolwin, K.: Surf. Sci. **287-288** (1993) 600.

- 93Kuc2 Kuch, W., Schulze, M., Schnurnberger, W., Bolwin, K.: Ber. Bunsenges. Phys. Chem. **97** (1993) 356.
- 93Laz Lazaga, M.A., Wickham, D.T., Parker, D.H., Kastanas, G.N., Koel, B.E.: ACS Symp. Ser. **523** (1993) 90.
- 93Mun Mundt, C., Benndorf, C.: Surf. Sci. **287-288** (1993) 119.
- 93Sha Shao, Y., Paul, J.: Appl. Surf. Sci. **72** (1993) 113.
- 93Sta Starke, U., Materer, N., Barbieri, A., Döll, R., Heinz, K., Van Hove, M.A., Somorjai, G.A.: Surf. Sci. **287-288** (1993) 432.
- 93Xu Xu, X., Vesecky, S.M., He, J.-W., Goodman, D.W.: J. Vac. Sci. Technol. A **11** (1993) 1930.
- 94Coe Coenen, F.P., Kästner, M., Pirug, G., Bonzel, H.P., Stimming, U.: J. Phys. Chem. **98** (1994) 7885.
- 94Gre Grellner, F., Klingenberg, B., Borgmann, D., Wedler, G.: Surf. Sci. **312** (1994) 143.
- 94Gri Griffiths, K., Kasza, R.V., Esposto, F.J., Callen, B.W., Bushby, S.J., Norton, P.R.: Surf. Sci. **307-309** (1994) 60.
- 94Hel1 Held, G., Menzel, D.: Surf. Sci. **316** (1994) 92.
- 94Hel2 Held, G., Menzel, D.: Proc. 4th Int. Conf. Struct. on Surf. **4** (1994) 213.
- 94Kuc Kuch, E., Schnurnberger, W., Schulze, M., Bolwin, K.: J. Chem. Phys. **101** (1994) 1687.
- 94Mil Miller, J.B., Bernasek, S.L., Schwartz, J.: Langmuir **10** (1994) 2629.
- 94Mun Mundt, C., Benndorf, C.: Surf. Sci. **307-309** (1994) 28.
- 94Oga Ogasawara, H., Yoshinobu, J., Kawai, M.: Chem. Phys. Lett. **231** (1994) 188.
- 94Pan Pangher, N., Schmalz, A., Haase, J.: Chem. Phys. Lett. **221** (1994) 189.
- 94Pir Pirug, G., Knauff, O., Bonzel, H.P.: Surf. Sci. **321** (1994) 58.
- 94Pol Polak, M.: Surf. Sci. **321** (1994) 249.
- 94Shi Shi, H., Jacobi, K.: Surf. Sci. **317** (1994) 45.
- 95Bau Baumann, P., Pirug, G., Reuter, D., Bonzel, H.P.: Surf. Sci. **335** (1995) 186.
- 95Ben Bensebaa, F., Ellis, T.H.: Prog. Surf. Sci. **50** (1995) 173.
- 95Bry Bryl, R., Wysocki, T., Blazczyszyn, R.: Appl. Surf. Sci. **87/88** (1995) 69.
- 95Cha1 Chakarov, D.V., Österlund, L., Kasemo, B.: Langmuir **11** (1995) 1201.
- 95Cha2 Chakarov, D.V., Österlund, L., Kasemo, B.: Vacuum **46** (1995) 1109.
- 95Chi1 Chia, W.J., Chung, Y.W.: Intermetallics **3** (1995) 505.
- 95Chi2 Chia, W.J., Chung, Y.W.: J. Vac. Sci. Technol. A **13** (1995) 1687.
- 95Gle Gleason, N.R., Chaturvedi, S., Strongin, D.R.: Surf. Sci. **326** (1995) 27.
- 95Gre Grellner, F., Klingenberg, B., Borgmann, D., Wedler, G.: J. Electron Spectrosc. Relat. Phenom. **71** (1995) 107.
- 95Hel1 Held, G., Menzel, D.: Phys. Rev. Lett. **74** (1995) 4221.
- 95Hel2 Held, G., Menzel, D.: Surf. Sci. **327** (1995) 301.
- 95Jac Jacobs, D.C.: J. Phys. Condens. Matter **7** (1995) 1023.
- 95Kiz Kizhakevariam, N., Villegas, I., Weaver, M.J.: J. Phys. Chem. **99** (1995) 7677.
- 95Mat Materer, N., Starke, U., Barbieri, A., Van Hove, M.A., Somorjai, G.A., Kroes, G.-J., Minot, C.: J. Phys. Chem. **99** (1995) 6267.
- 95Phe Phelps, R.B., Kesmodel, L.L., Kelley, R.J.: Surf. Sci. **340** (1995) 134.
- 95Rom Romm, L., Livneh, T., Asscher, M.: J. Chem. Society Faraday Trans. **91** (1995) 3655.
- 95Sch Schulze, M., Reißner, R., Bolwin, K., Kuch, W.: Fresenius J. Anal. Chem. **353** (1995) 661.
- 95Stu Stuve, E.M., Krasnopoler, A., Sauer, D.E.: Surf. Sci. **335** (1995) 177.
- 95Tra Trasatti, S.: Surf. Sci. **335** (1995) 1.
- 95Vil Villegas, I., Kizhakevariam, N., Weaver, M.: Surf. Sci. **335** (1995) 300.
- 96Chi Chia, W.J., Chung, Y.W.: J. Vac. Sci. Technol. A **14** (1996) 1614.
- 96Gil Gilarowski, G., Erley, W., Ibach, H.: Surf. Sci. **351** (1996) 156.
- 96Gle Gleason, N.R., Strongin, D.R.: J. Phys. Chem. **100** (1996) 18829.
- 96Gri Griffiths, K., Bonnett, D.: Surf. Sci. **177** (1986) 169.
- 96Jia Jiang, P., Zappone, M.W., Bernasek, S.L., Robertson, A.: J. Vac. Sci. Technol. A **14** (1996) 2372.
- 96Kas Kasza, R.V., Griffiths, K., Shapter, J.G., Norton, P.R., Harrington, D.A.: Surf. Sci. **356** (1996) 195.

- 96Koc Koch, M.H., Jakob, P., Menzel, D.: Surf. Sci. **367** (1996) 293.  
 96Liv Livneh, T., Romm, L., Asscher, M.: Surf. Sci. **351** (1996) 250.  
 96Mor Morgenstern, M., Michely, T., Comsa, G.: Phys. Rev. Lett. **77** (1996) 703.  
 96Rei Reißner, R., Wagner, N., Kuch, W., Schulze, M., Lorenz, M., Schnurnberger, W.: Proc. 11th World Hydrogen Energy Conf., Inter. Assio. for Hydrogen Energy, Coral Gables (1996) 2473.  
 96Sch Schick, M., Xie, J., Mitchell, W.J., Weinberg, W.H.: J. Chem. Phys. **104** (1996) 7713.  
 96Smi Smith, R.S., Huang, C., Wong, E.K.L., Kay, B.D.: Surf. Sci. **367** (1996) L13.  
 97Bry Bryl, R.: Vacuum **48** (1997) 333.  
 97Gle Glebov, A., Graham, A.P., Menzel, A., Toennies, J.P.: J. Chem. Phys. **106** (1997) 9382.  
 97Hof Hoffmann, W., Benndorf, C.: Surf. Sci. **377-379** (1997) 681.  
 97Ike Ikemiya, N., Gewirth, A.A.: J. Am. Chem. Soc. **119** (1997) 9919.  
 97Kam Kammler, T., Scherl, M., Kuppers, J.: Surf. Sci. **382** (1997) 116.  
 97Li1 Li, B., Griffiths, K., Zhang, C.S., Norton, P.R.: Surf. Sci. **384** (1997) 70.  
 97Li2 Li, B., Griffiths, K., Zhang, C.-S., Norton, P.R.: Surf. Sci. **370** (1997) 97.  
 97Mor Morgenstern, M., Müller, J., Michely, T., Comsa, G.: Z. Phys. Chem. **198** (1997) 43.  
 97Rub Ruby, C., Fusy, J., Alnot, M., Genin, J.-M., Ehrhardt, J.-J.: Thin Solid Films **311** (1997) 44.  
 97Smi Smith, R.S., Kay, B.D.: Surf. Rev. Lett. **4** (1997) 781.  
 97Sue Sueyoshi, T., Sasaki, T., Iwasawa, Y.: J. Phys. Chem. **101** (1997) 4648.  
 97Vil Villegas, I., Weaver, M.J.: J. Phys. Chem. B **101** (1997) 5842.  
 97Wan Wang, H., Biesecker, J.P., Iedema, M.J., Ellison, G.B., Cowin, J.P.: Surf. Sci. **381** (1997) 142.  
 98Kov Kovar, M., Kasza, R.V., Griffiths, K., Norton, P.R., Williams, G.P., Van Campen, D.: Surf. Rev. Lett. **5** (1998) 589.  
 98Löf Löfgren, P., Kasemo, B.: Catal. Lett. **53** (1998) 33.  
 98Mun Mundt, C., Benndorf, C.: Surf. Sci. **405** (1998) 121.  
 98Oga Ogasawara, H., Yoshinobu, J., Kawai, M.: RIKEN Rev. **17** (1998) 39.  
 98Pan Panja, C., Saliba, N., Koel, B.E.: Surf. Sci. **395** (1998) 248.  
 98Pir Pirug, G., Bonzel, H.P.: Surf. Sci. **405** (1998) 87.  
 98Ras Raschke, M.B., Madey, T.E.: Phys. Rev. B **58** (1998) 15832.  
 98Sco Scovell, D.L., Pinkerton, T.D., Finnlayson, B.A., Stuve, E.M.: Chem. Phys. Lett. **294** (1998) 255.  
 98Su Su, X., Lianos, L., Shen, Y.R., Somorjai, G.A.: Phys. Rev. Lett. **80** (1998) 1533.  
 99Bry Bryl, R., Blazczyszyn, R.: Vacuum **54** (1999) 103.  
 99Che Chen, N., Blowers, B., Masel, R.I.: Surf. Sci. **419** (1999) 150.  
 99Gle Glebov, A.L., Graham, A.P., Menzel, A.: Surf. Sci. **427-428** (1999) 22.  
 99Kin Kino, Y., Murakami, F., Yagyu, S., Yamamoto, S.: Jpn. J. Appl. Phys. Part 1 **38** (1999) 868.  
 99Liv Livingston, F.E., Smith, J.A., George, S.M.: Surf. Sci. **423** (1999) 145.  
 99Nak Nakamura, M., Shingaya, Y., Ito, M.: Chem. Phys. Lett. **309** (1999) 123.  
 99Oga Ogasawara, H., Yoshinobu, J., Kawai, M.: J. Chem. Phys. **111** (1999) 7003.  
 99Pin Pinkerton, V.K., Scovell, D.V., Johnson, A.L., Xia, B., Medvedev, V.K., Stuve, E.M.: Langmuir **15** (1999) 851.  
 99Pöl Pölzl, H., Zinka, F., Gleispach, D., Winkler, A.: Surf. Sci. **440** (1999) 196.  
 00Dvo Dvorak, J., Dai, H.-L.: J. Chem. Phys. **112** (2000) 923.  
 00Gib Gibson, K.D., Viste, M., Sibener, S.J.: J. Chem. Phys. **112** (2000) 9582.  
 00Kan Kang, Y.C., Milovancev, M.M., Clauss, D.A., Lange, M.A., Ramsier, R.D.: J. Nucl. Mater. **281** (2000) 57.  
 00Nak Nakamura, M., Ito, M.: Chem. Phys. Lett. **325** (2000) 293.  
 00Sco Scovell, D.L., Pinkerton, T.D., Medvedev, V.K., Stuve, E.M.: Surf. Sci. **457** (2000) 365.  
 00Ske Skelton, D.C., Tobin, R.G., Fisher, G.B., Lambert, D.K., DiMaggio, C.L.: J. Phys. Chem. **104** (2000) 548.  
 00Wan Wang, J., Chung, Y.W.: J. Phys. Chem. B **104** (2000)  
 01Jac1 Jacobi, K., Bedürftig, K., Wang, Y., Ertl, G.: Surf. Sci. **472** (2001)

- 01Jac2 Jacobi, K.: Electron work function of metals and semiconductors, in: *Physics of Covered Solid Surfaces*. Landolt-Börnstein III/42 A1. Bonzel, H. P. (ed.), Berlin: Springer-Verlag, 2001
- 01Lil Lilach, Y., Romm, L., Livneh, T., Asscher, M.: *J. Chem. Phys. B* **105** (2001) 2736.
- 01Mau Maus-Friedrichs, W., Gunhold, A., Frerichs, M., Kempter, V.: *Surf. Sci.* **488** (2001) 239.
- 01Nak Nakamura, M., Ito, M.: *Chem. Phys. Lett.* **335** (2001) 170.
- 01Suz Suzuki, T., Kurahashi, M., Yamauchi, Y.: *Surf. Sci.* **476** (2001) 63.
- 02Fei Feibelman, P.J.: *Science* **295** (2002) 99.
- 02Haq Haq, S., Harnett, J., Hodgson, A.: *Surf. Sci.* **505** (2002) 171.
- 02Hen Henderson, M.A.: *Surf. Sci. Rep.* **46** (2002) 1.
- 02Kan Kang, Y.C., Ramsier, R.D.: *Surf. Sci.* **519** (2002) 229.
- 02Kom Komeda, T., Fukidome, H., Kim, Y., Kawai, M., Sainoo, Y., Shigekawa, H.: *Proceedings of 7th International Conference on Nanometer-Scale Science and Technology and 21st Europe (2002)*
- 02Mit Mitsui, T., Rose, M.K., Fomin, E., Ogletree, D.F., Salmeron, M.: *Science* **297** (2002) 1850.
- 02Mor1 Morgenstern, K.: *Surf. Sci.* **504** (2002) 293.
- 02Mor2 Morgenstern, K., Rieder, K.-H.: *J. Chem. Phys.* **116** (2002) 5746.
- 02Nak Nakamura, M., Ito, M.: *Surf. Sci.* **502**- (2002) 144.
- 02Oga Ogasawara, H., Brena, B., Nordlund, D., Nyberg, M., Pelmenschikov, A., Pettersson, L.G.M., Nilsson, A.: *Phys. Rev. Lett.* **89** (2002) 276102/1.
- 03Amm Ammon, C., Bayer, A., Steinrück, H.-P., Held, G.: *Chem. Phys. Lett.* **377** (2003) 163.
- 03Ank Ankrah, S., Kang, Y.C., Ramsier, R.D.: *J. Phys.: Condens. Matter* **15** (2003) 1899.
- 03Bly Blyth, R.I.R., Searle, C., Tucker, N., White, R.G., Johal, T.K., Thompson, J., Barrett, S.D.: *Phys. Rev. B* **68** (2003) 205404.
- 03Den Denzler, D.N., Hess, C., Dudek, R., Wagner, S., Frischkorn, C., Wolf, M., Ertl, G.: *Chem. Phys. Lett.* **367** (2003) 618.
- 03Fei Feibelman, P.J.: *Phys. Rev. B* **67** (2003) 35420.
- 03Har Harnett, J., Haq, S., Hodgson, A.: *Surf. Sci.* **528** (2003) 15.
- 03Mic Michaelides, A., Alavi, A., King, D.A.: *J. Am. Chem. Soc.* **125** (2003) 2746.
- 03Mor Morgenstern, K., Nieminen, J.: *J. Chem. Phys.* **120** (2003) 10786.
- 03Pui Puisto, S.R., Leretholi, T.J., Held, G., Menzel, D.: *Surf. Rev. Lett.* **10** (2003) 487.
- 03Zal Zalkind, S., Polak, M., Shamir, N.: *Surf. Sci.* **529** (2003) 189.
- 04And Andersson, K., Nikitin, A., Pettersson, L.G.M., Nilsson, A., Ogasawara, H.: *Phys. Rev. Lett.* **93** (2004) 196101/1.
- 04Cer Cerda, J., Michaelides, A., Bocquet, M.-L., Feibelman, P.J., Mitsui, T., Rose, M.K., Fomin, E., Salmeron, M.: *Phys. Rev. Lett.* **93** (2004) 116101/1.
- 04Fei Feibelman, P.J.: *Chem. Phys. Lett.* **389** (2004) 92.
- 04Gre Grecea, M.L., Backus, E.H.G., Riedmüller, B., Eichler, A., Kleyn, A.W., Bonn, M.: *J. Phys. Chem. B* **108** (2004) 12575.
- 04Jae Jaegermann, W., Mayer, T.: *H/sub2/O and OH on semiconductors*, in: *Physics of Covered Solid Surfaces*. Landolt Börnstein III/42A4. Bonzel, H. P. (ed.), Berlin: Springer-Verlag, 2004
- 04Mic Michaelides, A., Ranea, V.A., de Andres, P.L., King, D.A.: *Phys. Rev. B* **69** (2004) 75409.
- 04Wei Weissenrieder, J., Mikkelsen, A., Andersen, J.N., Feibelman, P.J., Held, G.: *Phys. Rev. Lett.* **93** (2004) 196102/1.
- 05Fei Feibelman, P.J.: *Chem. Phys. Lett.* **410** (2005) 120.